

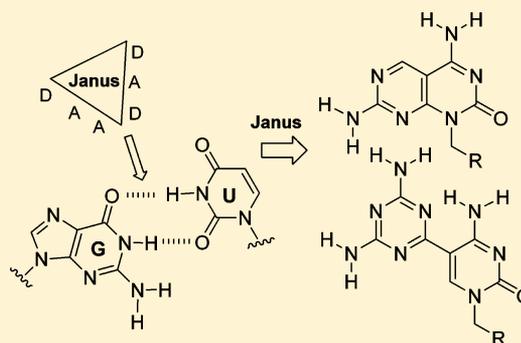
Synthesis of Janus Compounds for the Recognition of G-U Mismatched Nucleobase Pairs

Gerard Artigas and Vicente Marchán*

Departament de Química Orgànica, Facultat de Química, Universitat de Barcelona Martí i Franquès 1-11, E-08028 Barcelona, Spain

S Supporting Information

ABSTRACT: The design and synthesis of two Janus-type heterocycles with the capacity to simultaneously recognize guanine and uracyl in G-U mismatched pairs through complementary hydrogen bond pairing is described. Both compounds were conveniently functionalized with a carboxylic function and efficiently attached to a tripeptide sequence by using solid-phase methodologies. Ligands based on the derivatization of such Janus compounds with a small aminoglycoside, neamine, and its guanidinylated analogue have been synthesized, and their interaction with Tau RNA has been investigated by using several biophysical techniques, including UV-monitored melting curves, fluorescence titration experiments, and ^1H NMR. The overall results indicated that Janus-neamine/guanidinoneamine showed some preference for the +3 mutated RNA sequence associated with the development of some tauopathies, although preliminary NMR studies have not confirmed binding to G-U pairs. Moreover, a good correlation has been found between the RNA binding affinity of such Janus-containing ligands and their ability to stabilize this secondary structure upon complexation.



INTRODUCTION

Targeting RNA with small molecules, particularly human disease causing RNAs, has enormous potential in medicinal chemistry.¹ In addition to the notable case of compounds targeting bacterial rRNA,¹ recent examples have demonstrated that the function of other RNA sequences can be modulated with synthetic small molecules.² Similarly to proteins, RNA is able to fold local structural motifs such as stem loops, bulges or internal loops into complex three-dimensional architectures, thus generating targetable binding sites where ligands can be accommodated. The simultaneous recognition of such targetable motifs by compounds based on the combination of fragments is an attractive approach to develop ligands with increased RNA affinity and specificity.^{1,3} Moreover, this fragment-based approach might also be used to confer them with desirable druglike properties such as cellular permeability.⁴

Among the large variety of RNA structural motifs, the G-U wobble base pair⁵ plays an essential role in many biological processes, since it is recognized by proteins and other RNAs.⁶ Despite the fact that its thermodynamic stability is comparable to that of Watson–Crick base pairs, several studies have revealed that G-U wobble pairs are more prone to base opening than canonical pairs,⁷ which would facilitate their recognition through complementary hydrogen bond pairing by using nicknamed Janus-type molecules. Named after the two-faced Roman god, Janus-type heterocycles have two hydrogen bonding arrays complementary to the faces of a given pair of nucleobases.⁸ Insertion of such compounds between the two nucleobases is expected to provide higher affinity and specificity, since the number of hydrogen bonds will be

increased. Most of the Janus molecules reported have been incorporated into DNA, PNA analogues or peptides with negatively charged backbones with the aim of forming triplex or duplex structures upon bifacial recognition of target nucleobases.⁹ Diaminotriazine conjugation to an acridine derivative has also been explored for targeting U-U mismatch sites in CUG repeats in RNA associated with the development of myotonic dystrophy type 1 disease.¹⁰

Of current interest to our laboratory¹¹ is the development of ligands for the RNA secondary structure located at the exon 10-5' intron junction of Tau pre-mRNA, since it has been proposed as a therapeutic target for the treatment of several tauopathies, including frontotemporal dementia with parkinsonism linked to chromosome 17 (FTDP-17).^{12,13} Interestingly, wild-type Tau RNA has two G-U pairs (G+5 and G-4), and some of the disease-causing mutations (+13, +14, and +16) found in FTDP-17 patients form additional G-U pairs (see Figure 1) that diminish the thermodynamic stability of the stem-loop structure. This modifies exon 10 alternative splicing, and as a consequence, the correct ratio of tau protein isoforms is altered, which leads to dementia.¹⁴ Significantly, early NMR studies reported by Varani et al.^{12a} suggested that wobble G-U pairs are only formed in the case of +13 and +14 mutated sequences, whereas G-1 (+16 mutated sequence) and G+5 and G-4 (wt, +3 and +16) are not paired with their faced U's. On the basis of these precedents, we have envisaged that such G-U pairs might be used to selectively target Tau RNA with Janus-

Received: August 1, 2013

Published: October 2, 2013

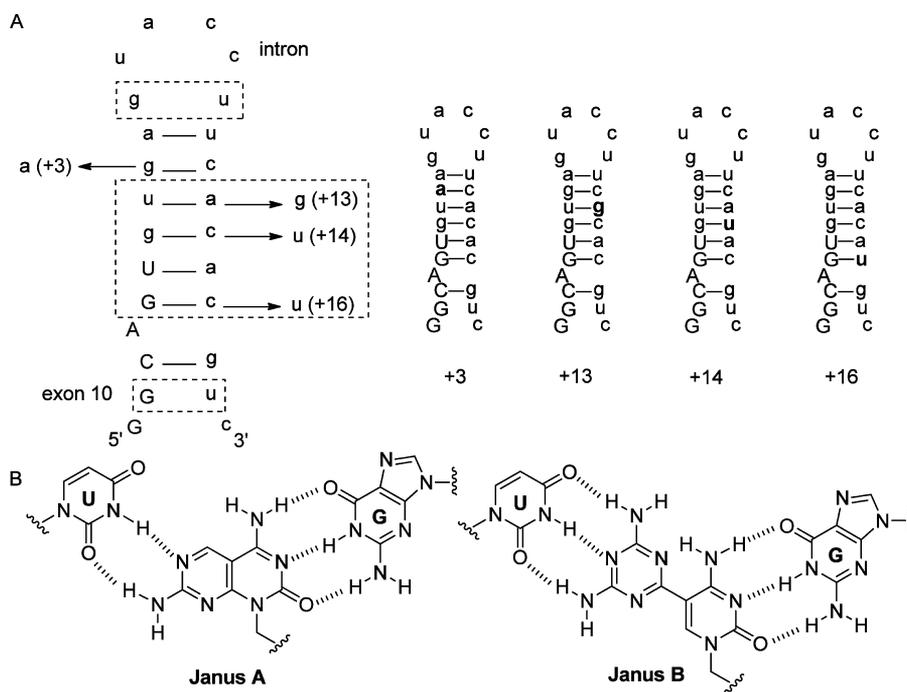
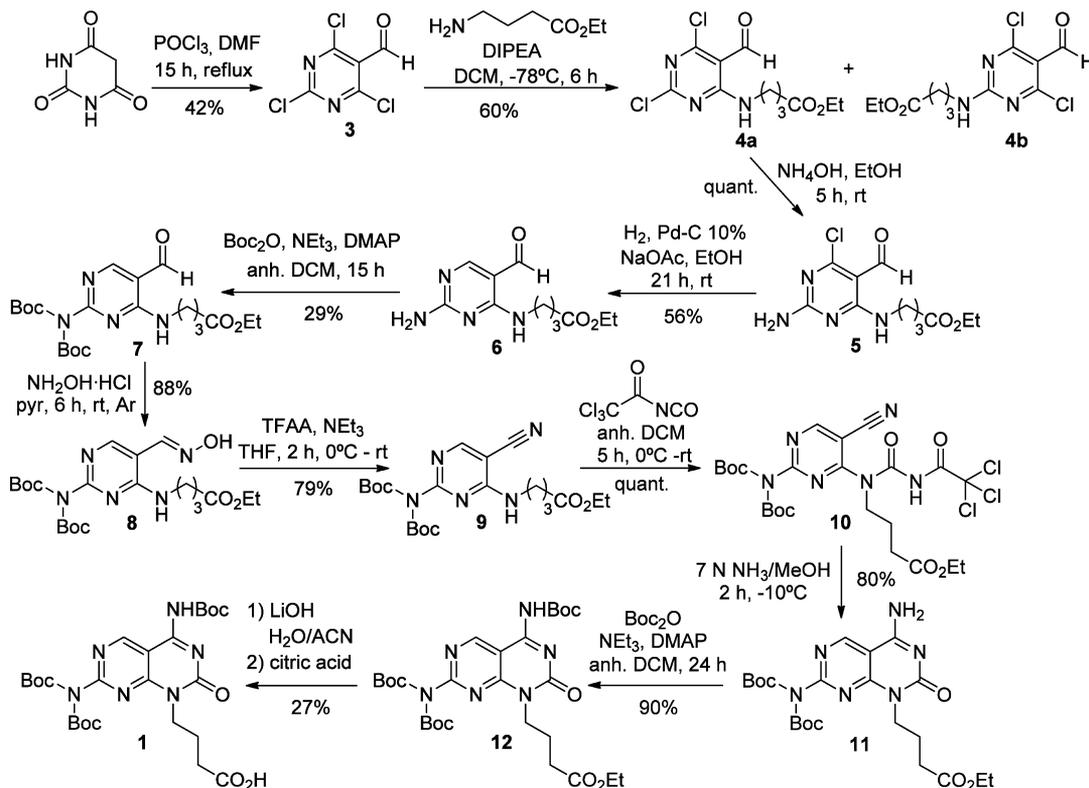


Figure 1. (A) Sequences and secondary structure of wild-type (wt) and +3, +13, +14 and +16 mutated Tau stem-loop RNAs. Exonic sequences are shown in capital letters and intronic sequences in lower case. Nucleotides involved in base pairs identified previously by NMR are connected by a dash.^{12a,13c} (B) Schematic representation of Janus A and Janus B heterocycles binding to G-U mismatched pairs.

Scheme 1. Synthesis of Janus A Monomer (1)



type molecules designed to recognize both mismatched nucleobases (Figure 1). It is expected that stabilization of the mutated RNA sequences upon ligand binding might allow the physiological balance of tau isoforms to be restored and consequently the tauopathy to be treated.^{11–14} We report herein the design and synthesis and, to the best of our

knowledge, the first Janus-type molecules (denoted in this work as Janus A and Janus B) capable of hydrogen bonding to G's and U's in G-U mismatched pairs. Ligands based on the derivatization of such Janus compounds with a small aminoglycoside, neamine, and its guanidinylated analogue have been

synthesized, and their interaction with Tau RNA has been investigated by using several biophysical techniques.

RESULTS AND DISCUSSION

Synthesis and Characterization of Janus Building Blocks 1 and 2. As shown in Figure 1, the heteroaromatic bicyclic Janus A molecule contains donor–acceptor–acceptor and acceptor–donor H-bond arrays. With regard to the Janus B molecule, we chose to incorporate both faces in separate aryl rings linked through a single bond, which might confer some degree of rotational flexibility. It should be noted that the formation of an intramolecular H bond between the exocyclic amino function of cytosine and the adjacent nitrogen of the diaminotriazine heterocycle might serve to keep it planar and semirigid, which might be important for recognition of G-U mismatched pairs. In this case, the diaminopurine face (donor–acceptor–donor H-bond array) was chosen to afford three Watson–Crick hydrogen bonds upon binding to uracyl, whereas the cytosine face (donor–acceptor–acceptor H-bond array) can form the three typical Watson–Crick hydrogen bonds with guanine, as in Janus A. Hence, Janus A and Janus B containing compounds might have the potential to form five or six hydrogen bonds with G-U mismatched pairs, respectively. Since the final aim is to combine such Janus structures with other molecules such as peptides and glycosides to generate ligands with increased RNA specificity, we planned the synthesis of two Janus monomers (compound 1 for Janus A in Scheme 1 and compound 2 for Janus B in Scheme 2) with a carboxylic function to allow further derivatization in solution or in a solid phase through the formation of an amide bond.

Compound 1 was prepared in 11 steps and 68% average stepwise yield (Scheme 1). First, barbituric acid was converted into 2,4,6-trichloropyrimidine-5-carbaldehyde (3) by a Vilsmeier reaction with phosphorus oxychloride and DMF.¹⁵ Nucleophilic aromatic substitution with ethyl aminobutyrate (1 mol equiv) at 0 °C in the presence of triethylamine afforded simultaneous substitution at positions 2 and 4 in the pyrimidine ring. Although monosubstitution at position 4 was favored at low temperature (–78 °C), MS analysis showed the formation of several side products because of the nucleophilic attack of triethylamine. This side reaction was minimized by using a sterically hindered base, *N,N*-diisopropylethylamine, which gave compound 4a in 60% yield after flash column chromatography. This compound differs from its regioisomer 4b (*S_NAr* at position 2) in the ¹H NMR chemical shift of the amino function (δ 9.36 ppm for 4a and δ 6.28 ppm for 4b). 1D NOE irradiation of the proton at 9.36 ppm showed a clear NOE enhancement of the aldehyde proton, whereas that phenomenon did not occur for the proton at 6.28 ppm, which allowed the unambiguous distinction of both isomers.

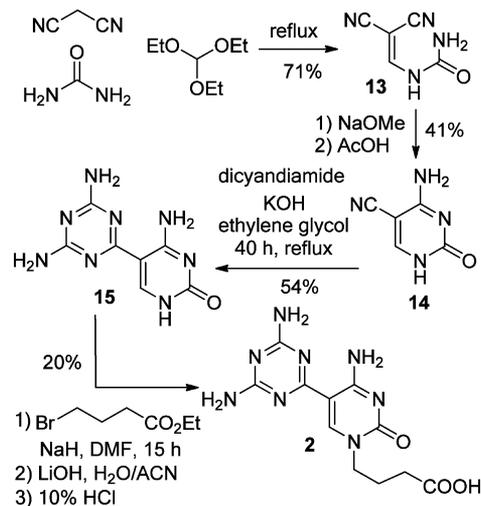
A second nucleophilic aromatic substitution with aqueous ammonia afforded compound 5 in quantitative yield. It is interesting to note that *S_NAr* occurs exclusively at position 2 when the reaction is carried out at room temperature for 5 h, whereas a large excess of ammonia and higher temperature gives substitution at positions 2 and 6. Similar results have been reported with other derivatives of 2,6-dichloropyrimidine that contain an amino substituent at position 4 and electron-withdrawing groups (aldehyde or ester) at position 5 of the ring.^{15b,c,16,17}

The next step was the reduction of the aryl chloride group by H₂ with 10% Pd–C in the presence of sodium acetate, which afforded 6 in 56% yield after chromatographic purification.

Notably, the aldehyde group was not reduced under the conditions used for carrying out catalytic hydrogenation. The primary amino function was bis-Boc protected by reaction with *tert*-butoxycarbonyl anhydride in DMF in the presence of a catalytic amount of DMAP. In addition to 7 (29% yield after purification), several side products were identified, including those derived from monoprotection of both amino functions. Then, the aldehyde was transformed to oxime 8 in 88% yield, and dehydration with trifluoroacetic anhydride produced the fluorescent nitrile derivative 9 (79%). The critical step of the synthesis route involved the transformation of the free secondary amino function into an activated urea derivative to allow cyclization in basic media. To our surprise, this aromatic amine function was found to be very unreactive, since no evidence of reaction was obtained when using triphosgene, phosgene, trimethylsilyl isocyanate, or chlorosulfonyl isocyanate. Reaction with *N*-chlorocarbonyl isocyanate^{15b} at –10 °C in the presence of triethylamine afforded in very low yield the *N*-chlorocarbonylurea derivative. Finally, reaction with trichloroacetyl isocyanate at 0 °C in anhydrous DCM under an Ar atmosphere produced compound 10 in nearly quantitative yield after flash column chromatography. Cyclization in a concentrated methanolic solution of ammonia afforded the key compound (11, 80% yield) that contains both Janus faces. Boc protection of the free amino group followed by basic hydrolysis of the ester yielded the final Janus A monomer 1 as a clear yellow solid, which was fully characterized by HR-ESI MS and ¹H and ¹³C NMR.

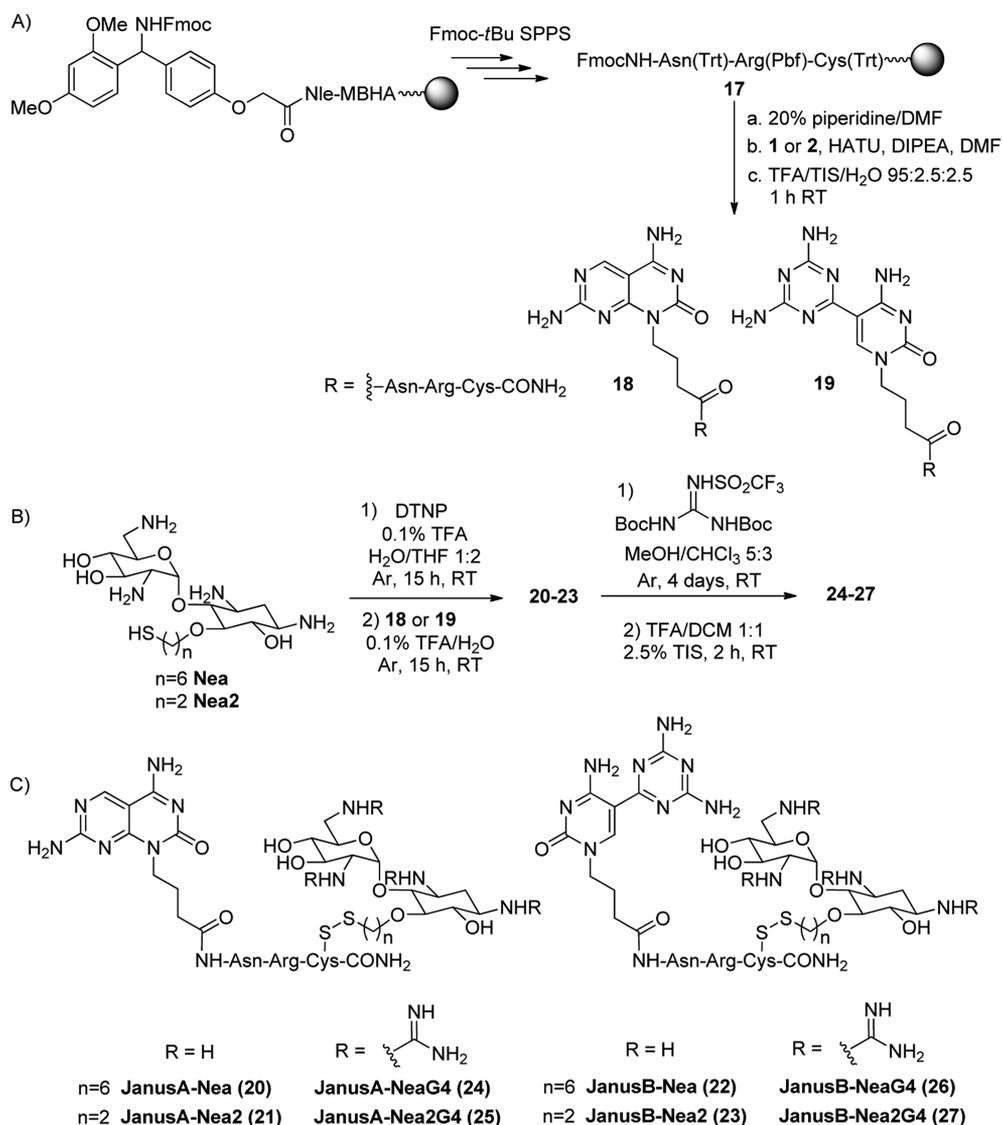
Compound 2 was prepared in four steps and 47% average stepwise yield (Scheme 2) from malononitrile, urea, and

Scheme 2. Synthesis of Janus B Monomer (2)



triethyl orthoformate. The key step involved the condensation of the nitrile group of 5-cyanocytosine¹⁸ with dicyandiamide¹⁹ in dry ethylene glycol in the presence of KOH at 150 °C for 40 h, which afforded 15 as a brown solid in 54% yield. Mild condition reactions, such as those reported for the construction of diaminotriazine from 5-cyanouracyl,^{19c} failed in this case, and more energetic conditions were required (e.g., prolonged heating at 150 °C or assistance by microwave irradiation). The next step involved alkylation of N1 of the cytosine ring with ethyl bromobutyrate by using NaH in DMF. Hydrolysis of the intermediate with LiOH afforded the expected Janus B monomer (2). According to previous studies on the

Scheme 3. Synthesis of Janus-Neamine/Guanidinoneamine Ligands: (A) Solid-Phase Synthesis of Thiol-Containing Janus-Peptide Derivatives; (B) Synthesis; (C) Structure of Janus-Containing Ligands



incorporation of triazine-containing amino acids onto peptides by solid-phase methodologies,²⁰ we decided not to protect the amino groups of the triazine moiety. Interestingly, ¹H NMR spectra of compound 2 suggests the formation of an intramolecular hydrogen bond between the exocyclic amino group of cytosine and N2 of the triazine ring, which might protect it from acylation during amide bond formation.

Synthesis and Characterization of Janus-Containing Ligands. Targeting G-U mismatched pairs in Tau RNA or in other RNA secondary structures with Janus-type molecules requires conferring them with the capacity to selectively recognize RNA from DNA. Aminoglycosides fulfill this requirement, since they are able to discriminate A-type from B-type duplexes and have relatively high affinity for RNA.²¹ However, these natural antibiotics lack RNA sequence specificity; thus, they are considered promiscuous compounds. In spite of this drawback, aminoglycosides are privileged building blocks for designing new RNA ligands.²² Recently, we have described a series of ligands for Tau RNA based on the combination of neamine and its guanidylated analogue, guanidinoneamine, with heteroaromatic compounds such as

acridines and an azaquinolone derivative with the capacity to recognize unpaired adenines.¹¹ On the basis of these precedents, our next objective was the derivatization of Janus A and B heterocycles with these small glycosides. It is worth noting that replacement of the amino functions of neamine by guanidinium groups is expected to improve uptake by eukaryotic cells, as well as the RNA binding affinity and stabilizing capacity of the ligands.²³ The synthesis of the ligands and their structures are shown in Scheme 3. Since the distance between both building blocks can be a critical parameter in ligands based on the combination of fragments, we used two thiol-containing neamine derivatives (Nea and Nea2)¹¹ differing in the length of the spacer between the thiol group and the glycoside core.

First, both Janus heterocycles were derivatized with a cysteine-containing peptide, since the reactive thiol group was planned to be used for the attachment to the aminoglycoside via the formation of a disulfide linkage. Moreover, the guanidinium and carboxamide groups provided by arginine and asparagine, respectively, could generate additional interactions with RNA (e.g., hydrogen bonding and/or electro-

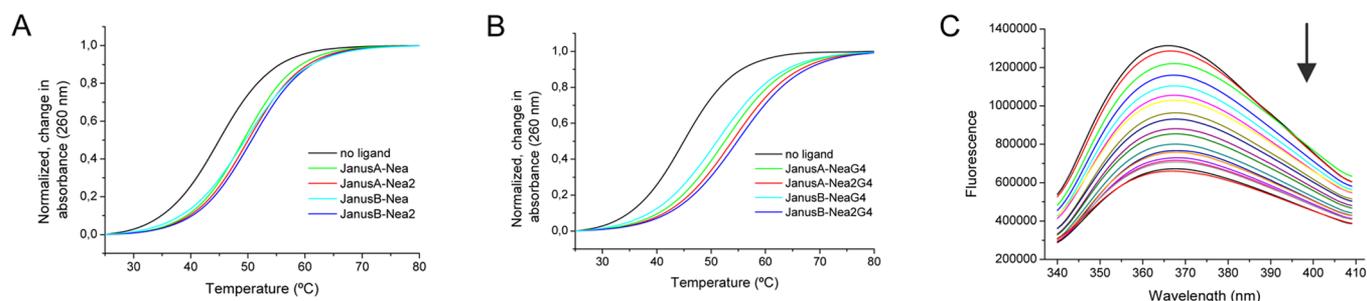


Figure 2. UV melting profiles for the +3 mutated RNA sequence and its ligand complexes with (A) Janus-neamine and (B) Janus-guanidinoneamine ligands at a [ligand]/RNA ratio of 1.0. (C) Fluorescence quenching of +3 RNA labeled with 2-aminopurine-2'-deoxyribonucleotide in the loop upon addition of increasing concentrations of Janus B-Nea2. Measurements were performed with an RNA concentration of 83 nM and ligand concentrations ranging from 0 to 5.43 μ M in 10 mM pH 6.8 sodium phosphate buffer, 50 mM NaCl, and 0.1 mM Na_2EDTA .

static). The tripeptide was assembled on a Rink amide *p*-MBHA resin using standard Fmoc/tBu chemistry. Janus monomers **1** and **2** were efficiently attached into the N terminus of the peptide by using HATU as a coupling reagent. Cleavage and deprotection with TFA/TIS/ H_2O 95:2.5:2.5 for 1 h at room temperature afforded the target compounds (**18** and **19**; Scheme 3) with high purity according to HPLC analysis. This confirms that it is not necessary to protect the exocyclic amino function of cytosine in monomer **2**.

Janus-neamine ligands **20–23** were easily synthesized in a two-step process which implicates two consecutive thiol–disulfide exchange reactions. First, thiol-derivatized neamine monomers Nea and Nea2¹¹ were activated with 2,2'-dithiobis-(5-nitropyridine) (DTNP)²⁴ under acidic conditions for 15 h under an Ar atmosphere. Then, the disulfide intermediates were reacted with the thiol-containing Janus-peptide monomers **18** and **19**, which afforded the desired ligands **20–23** after purification by reversed-phase HPLC (yields 21–53%). All of the compounds were fully characterized by NMR (1D ^1H , COSY, TOCSY) and high-resolution ESI mass spectrometry.

As shown in Scheme 3, the guanidylated ligands **24–27** were prepared by direct guanidinylation of their precursors **20–23** following previously reported procedures.^{11b,25} A 40-fold molar equivalent excess of *N,N'*-di-Boc-*N''*-triflylguanidine in the presence of triethylamine (240 mol equiv) was used in all cases. After acidic deprotection and purification by HPLC, Janus-guanidinoneamine ligands were obtained (yields: 23–25%) and characterized by NMR and HRMS. A significant amount of the triguanidylated ligand was also isolated, which indicates that the guanidinylation reaction did not reach completion after 4 days.

Studies on the Interaction of Janus-Containing Ligands with Tau RNA. Our next objective was to study the interaction of Janus-neamine ligands **20–23** and their guanidylated derivatives, Janus-guanidinoneamine **24–27**, with Tau RNA, and in particular to evaluate their ability to stabilize the RNA target. In addition to wt we chose two of the mutated sequences associated with the development of tauopathies, +3 and +16. As previously mentioned, all of them contain two G-U mismatched pairs and +16 mutation generates an additional G-U mismatched pair adjacent to the bulged adenine. UV melting experiments were carried out by monitoring the absorbance at 260 nm as a function of temperature, which allowed us to determine the melting temperature (T_m) as indicative of the thermal stability of the RNA secondary structure (Figure 2). ΔT_m values in Table 1

show the effect of the ligands on the T_m value of RNA upon complexation.

Table 1. Melting Temperatures (T_m , °C) for the Complexation of the Ligands with Tau RNAs^a

	T_m (wt)	ΔT_m^b	T_m (+3)	ΔT_m^b	T_m (+16)	ΔT_m^b
no ligand	63.0		44.3		56.6	
neamine	62.8	−0.2	48.1	+3.8	56.8	+0.2
Janus A-Nea	63.1	+0.1	49.3	+5.0	58.5	+1.9
Janus A-Nea2	63.6	+0.6	50.4	+6.1	57.6	+1.0
Janus B-Nea	62.8	−0.2	49.6	+5.3	58.0	+1.4
Janus B-Nea2	63.4	+0.4	50.4	+6.1	57.6	+1.0

^aConditions: 1 μ M both in RNA and in ligands in 10 mM pH 6.8 sodium phosphate buffer, 50 mM NaCl, 0.1 mM Na_2EDTA . ^b $\Delta T_m = (T_m \text{ of the RNA in the presence of ligand}) - (T_m \text{ of RNA alone})$.

As shown in Table 1, the effect of Janus-neamine ligands on the thermal stability of wt RNA was almost negligible, being similar to that obtained with the free aminoglycoside. However, this effect was positive in the case of the mutated sequences, being particularly higher with the +3 mutant. Interestingly, the effect of the length of the spacer linking both fragments was different, depending on the nature of the RNA sequence: a shorter spacer caused a greater increase in the T_m values for +3 RNA ($\Delta T_m = +5.0$ °C for JanusA-Nea vs $\Delta T_m = +6.1$ °C for JanusA-Nea2), whereas the opposite tendency was found for +16 RNA ($\Delta T_m = +1.9$ °C for JanusA-Nea vs $\Delta T_m = +1.0$ °C for JanusA-Nea2). This suggests that the binding site of these compounds might be different, depending on the secondary structure of the RNA target. To our surprise, the stabilizing ability of the ligands was independent of the nature of the Janus-type heterocycle. However, the fact that the T_m values of Janus-neamine ligands were slightly higher than those of neamine alone with +3 and +16 RNAs seems to suggest that the Janus-peptide fragment might participate in RNA binding. Moreover, the higher stabilization of +3 RNA in comparison with that of +16 (e.g., JanusA-Nea2, $\Delta T_m = +6.1$ °C for +3 vs $\Delta T_m = +1.0$ °C for +16) might be a consequence of some kind of selectivity for this RNA mutated sequence.

These results prompted us to evaluate the ability of Janus-guanidinoneamine ligands **24–27** to stabilize the +3 mutated sequence. As shown in Table 2, guanidinylation of the aminoglycoside moiety in Janus-neamine ligands always had a positive effect on the thermal stability of the RNA upon complexation. This effect was particularly important in the two ligands with the shorter spacer independent of the Janus

Table 2. Melting Temperatures (T_m , °C) for the Complexation of Ligands with Target RNAs^a

	$T_m(+3)$	ΔT_m^b	$\Delta T_m(G)^c$
no ligand	44.3		
guanidinoneamine	50.1	+5.8	+2.0
Janus A-NeaG4	52.6	+8.3	+3.3
Janus A-Nea2G4	54.2	+9.9	+3.8
Janus B-NeaG4	51.0	+6.7	+1.4
Janus B-Nea2G4	54.2	+9.9	+3.8

^aConditions: 1 μ M both in RNA and in ligands in 10 mM pH 6.8 sodium phosphate buffer, 50 mM NaCl, 0.1 mM Na₂EDTA. ^b $\Delta T_m = (T_m \text{ of the RNA in the presence of ligand}) - (T_m \text{ of RNA alone})$. ^c $\Delta T_m(G) = (T_m \text{ of the RNA in the presence of the guanidylated ligand}) - (T_m \text{ of the RNA in the presence of the parent non-guanidylated ligand})$.

heterocycle ($\Delta T_m(G) = +3.8$ °C for JanusA-Nea2G4 and JanusB-Nea2G4). However, the additional stabilization provided by the guanidinium groups was lower in the case of the ligand with the longer spacer that contains the Janus B heterocycle (e.g., $\Delta T_m(G) = +3.3$ °C for Janus A-NeaG4 vs $\Delta T_m(G) = +1.4$ °C for Janus B-NeaG4).

In order to check if the guanidylated derivatives have binding affinities higher than those of their parent amino compounds, quantitative binding studies were carried out by fluorescence titration experiments with the +3 mutated RNA since, as previously mentioned, T_m values suggested some preference for this oligoribonucleotide sequence. On the basis of previous studies with other Tau RNA ligands,¹¹ we decided to label +3 Tau RNA with fluorescein, since a characteristic dose-dependent saturable quenching in the fluorescence of the RNA is usually observed upon complexation with the ligands.²⁶ This approach allows EC_{50} values (the effective ligand concentration required for 50% RNA response) to be obtained by fitting the data to a sigmoidal dose–response curve. To our surprise, upon addition of increasing concentrations of Janus-containing ligands, either Janus A or Janus B, the fluorescence intensity of the fluorescein-labeled RNA increased (upon excitation at 490 nm) and the maximum was shifted from the typical 517 nm value to 522–525 nm. This behavior might be attributed to the presence of several binding sites in the RNA structure or to the interaction of the ligands with fluorescein.²⁶ As an alternative to fluorescein, we choose the fluorescent nucleotide analogue 2-aminopurine-2'-deoxyribonucleotide (2-AP), which has also been widely used to determine binding affinities for RNA.²⁷ In order to minimize alterations in the structure and stability of +3 Tau RNA, we decided to replace the adenine base of the loop with 2-AP. Again, changes in 2-AP fluorescence intensity upon excitation at 290 nm were measured as a function of the concentration of the ligands. Unfortunately, the inherent fluorescence of the Janus A heterocycle hampered the accurate determination of EC_{50} values for Janus A containing ligands. However, the binding affinities of the four Janus B containing ligands (Table 3) could be determined with 2-AP-labeled +3 RNA. As shown in Figure 2, the fluorescence of 2-AP decreased upon addition of increasing concentrations of the ligands, while the wavelength of the fluorescence maximum stayed constant. In this case, the inherent fluorescence of the ligand could be efficiently subtracted from that of the labeled RNA by repeating the full titration in the absence of RNA. Two main conclusions can be drawn from the EC_{50} values reported in Table 3. First, the

Table 3. Binding of the Ligands to +3 RNA

ligand	EC_{50} (nM) ^a
Janus B-Nea	296.7 \pm 63
Janus B-NeaG4	216.2 \pm 20
Janus B-Nea2	213.4 \pm 45
Janus B-Nea2G4	122.8 \pm 19

^aAll fluorescence measurements were performed in 10 mM pH 6.8 sodium phosphate buffer, 50 mM NaCl, and 0.1 mM Na₂EDTA.

binding affinities of the ligands are relatively high (120–300 nM) and the length of the spacer seems to be a critical parameter, since the binding was observed to be stronger for the ligands containing the shorter spacer linking both fragments, independent of the glycoside moiety ($EC_{50} = 296$ nM for Janus B-Nea vs $EC_{50} = 213$ nM for Janus B-Nea2). Second, guanidinylation of the aminoglycoside had a positive influence on binding affinity, which was slightly higher in the case of the ligand with the shorter spacer ($EC_{50} = 213$ nM for Janus B-Nea2 vs $EC_{50} = 122$ nM for Janus B-Nea2G4).

Altogether, these results show a good correlation between binding affinities of Janus B containing ligands and their ability to stabilize Tau RNA. Indeed, the T_m values of +3 RNA were increased in the presence of the ligands that had shown higher binding affinities. Although binding affinities could not be determined for Janus A containing ligands, according to T_m values reported in Tables 1 and 2, it is expected for these compounds to have EC_{50} values similar to those of Janus B containing ligands.

Finally, preliminary NMR studies were carried out to check if Janus-containing ligands can recognize G-U mismatched pairs through the formation of complementary hydrogen bonds. Due to the lack of a well-defined structure for the +3 mutated sequence, we choose wt RNA as a model for studying the effect of ligand addition on its 1D ¹H NMR spectra, particularly on the imino and aromatic regions. The structures of this oligoribonucleotide and its complexes with neomycin and mitoxantrone have been studied by Varani et al.,^{12a,13c} and they can be used as references for interpreting changes in the NMR spectra of Tau RNA in the presence of Janus-containing ligands. As shown in Figure 3, the addition of Janus A-Nea2 or Janus B-Nea2 caused a general line broadening of all signals but no significant changes in the chemical shifts of the imino protons. For example, the imino resonance of G+1 (δ 12.65 ppm) and G–1 (δ 12.84 ppm) were slightly shifted in both RNA-ligand complexes (δ 12.55 and 12.78 ppm, respectively), whereas U0 and U+2 imino resonances collapsed into a single broad signal. Additionally, changes of the chemical shifts at fields higher than that for the imino resonances, particularly in the region between 5.5 and 8.5 ppm, might be attributed to nonexchangeable groups of the neamine moiety. Interestingly, a new signal around δ 9.55 ppm (relative integration 1) appeared in the case of the Janus B-Nea2 ligand. Taken together, these effects on the NMR spectra suggest that Janus-type heterocycles, either Janus A or Janus B, do not seem to bind any of the two G-U mismatched pairs in wt RNA, since no new imino signals are formed in the region between 10 and 14 ppm. However, small changes in the chemical shifts of the imino resonances in the upper helical region (e.g., G–1, U0, G+1, and U+2) might be related to electrostatic and/or hydrogen bond interactions with RNA through the major groove, in a way similar to that of neomycin.^{13a} However, we cannot rule out the

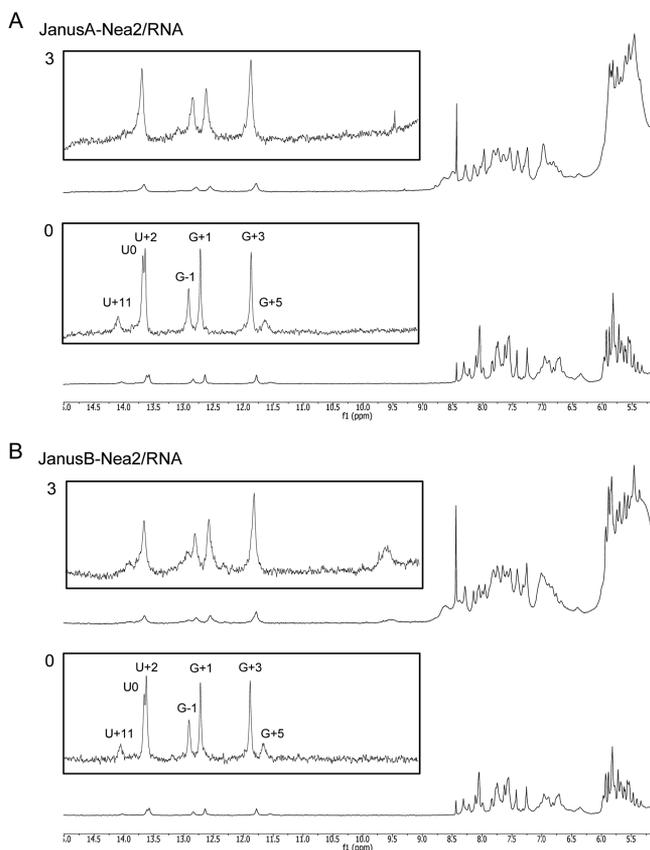


Figure 3. Region of the NMR spectra of wt RNA alone and in the presence of 3 mol equiv of Janus A-Nea2 (A) or Janus B-Nea2 (B) ligands. Imino proton signals are labeled according to the numbering scheme shown in Figure 1. Assignments were taken from Varani et al.^{12a,13c} The RNA concentration was 40 μ M in a 10 mM pH 6.8 sodium phosphate buffer, in a 90%/10% H₂O/D₂O mixture ($T = 5$ °C).

formation of selective hydrogen bonds between Janus-type heterocycles and other RNA nucleobases.

CONCLUSION

In summary, two Janus-type heterocycles with the capacity to recognize guanine and uracil in G-U mismatched pairs through complementary hydrogen bond pairing have been described. The key step in the synthesis of Janus A monomer (11 steps, 68% average stepwise yield) involved the use of trichloroacetyl isocyanate, which allowed cyclization of the intermediate to generate both fused faces. In the case of Janus B monomer (4 steps, 47% average stepwise yield), condensation of 5-cyanocytosine and dicyandiamine under energetic conditions was necessary to generate the diaminotriazine ring. Both compounds were conveniently derivatized with a cysteine-containing tripeptide by using solid-phase methodologies. Thiol–disulfide exchange reactions on a solution phase were used for the assembly of Janus-neamine ligands differing in the length of the spacer linking the Janus moiety and the aminoglycoside. Their guanidylated derivatives, Janus-guanidinoneamine ligands, were also prepared directly by guanidinylation of their amino parent compounds. All Janus-containing ligands were able to stabilize two mutated sequences associated with the development of FTDP-17, particularly the +3 sequence. Moreover, ligands containing the Janus B fragment bind this RNA sequence with high affinity ($EC_{50} = 120$ – 300

nM), showing a good correlation between binding affinity and their stabilizing properties. Although no evidence for the formation of hydrogen bonds between the Janus heterocycles and wt RNA can be deduced from 1D ¹H NMR titration experiments, changes in some chemical shifts confirm binding to this target. Efforts are underway to study by NMR spectroscopy the structure of the +3 mutated RNA sequence and their complexes with Janus-containing ligands to determine if the higher stabilizing ability of these compounds with respect to this RNA target is related to the recognition of G-U mismatched pairs by Janus heterocycles. Furthermore, these Janus-type building blocks might be used in the future to develop specific ligands for targeting G-U pairs in other human disease causing RNAs.

EXPERIMENTAL SECTION

Unless otherwise stated, common chemicals and solvents (HPLC grade or reagent grade quality) were purchased from commercial sources and used without further purification. Aluminum plates coated with a 0.2 mm thick layer of silica gel 60 F₂₅₄ were used for thin-layer chromatography analyses (TLC), whereas flash column chromatography purification was carried out using silica gel 60 (230–400 mesh). Reversed-phase high-performance liquid chromatography (HPLC) analyses of the compounds were carried out on a Jupiter Proteo C₁₈ column (250 × 4.6 mm, 90 Å 4 μ m, flow rate 1 mL/min) using linear gradients of 0.045% TFA in H₂O (solvent A) and 0.036% TFA in ACN (solvent B). Semipreparative purification was carried out in a Jupiter Proteo column (250 × 10 mm, 10 μ m, flow rate 3 mL/min), using linear gradients of 0.1% TFA in H₂O (solvent A) and 0.1% TFA in ACN (solvent B). After several runs, pure fractions were combined and lyophilized.

NMR spectra were recorded at 25 °C on different spectrometers (300, 400, 500, or 600 MHz) using deuterated solvents. Tetramethylsilane (TMS) was used as an internal reference (0 ppm) for ¹H spectra recorded in CDCl₃, and the residual signal of the solvent (77.16 ppm) was used for ¹³C spectra. For DMSO-*d*₆, the residual signal of the solvent was used as a reference in ¹H and ¹³C spectra. Chemical shifts are reported in parts per million (ppm) in the δ scale, coupling constants in Hz, and multiplicities as follows: s (singlet), d (doublet), t (triplet), q (quadruplet), qt (quintuplet), m (multiplet), td (doublet of triplets), br (broad signal).

Electrospray ionization mass spectra (ESI-MS) were recorded on an instrument equipped with a single-quadrupole detector coupled to an HPLC, and high-resolution (HR) ESI-MS were recorded on an LC/MS-TOF instrument.

Synthesis of Janus A Monomer (1). 2,4,6-Trichloropyrimidine-5-carbaldehyde (**3**). Barbituric acid (30 g, 0.234 mol) was slowly added to a stirred solution of POCl₃ (140 mL, 1.51 mol) in DMF (25 mL, 0.234 mol) at room temperature under Ar, and the mixture rapidly acquired a yellow color. After it was refluxed for 15 h, the mixture was cooled to room temperature and evaporated in vacuo to remove most of the POCl₃ excess. Then, the residue was carefully poured over crushed ice while vigorous stirring was maintained, and the resulting brown precipitate was filtered and dried under vacuum. After flash column chromatography (gradient 0–50% AcOEt in hexane), the desired product was obtained as a brown solid (21 g, 42%) and used in the next step without further purification. TLC: R_f (10% AcOEt/hexane) 0.43. Mp: 166–169 °C. ¹H NMR (400 MHz, CDCl₃; δ (ppm)): 10.42 (1H, s). ¹³C NMR (100 MHz, CDCl₃; δ (ppm)): 184.8, 164.2, 161.8, 123.2.

Ethyl 4-((2,6-Dichloro-5-formylpyrimidin-4-yl)amino)butanoate (4a). To a stirred solution of **3** (10 g, 47.3 mmol) in DCM (200 mL) was slowly added a solution of ethyl 4-aminobutyrate hydrochloride (7.92 g, 47.3 mmol) and DIPEA (16.1 mL, 94.6 mmol) in DCM (100 mL) at –78 °C under an Ar atmosphere. The resulting mixture, which immediately acquired a yellow color, was stirred at –78 °C for 6 h. Once at room temperature, the reaction mixture was taken up and washed with water (2 × 50 mL) and brine

(50 mL). The resulting organic phase was dried over anhydrous MgSO_4 , filtered, and concentrated in vacuo to dryness. After flash column chromatography (gradient 2.5–20% AcOEt in hexane), the desired compound (**4a**) was obtained as a yellow crystalline solid (8.53 g, 60%). In addition, regioisomer **4b** was also isolated as a minor product. Data for **4a** are as follows. TLC: R_f (20% AcOEt/hexane) 0.37. Mp: 91–93 °C. ^1H NMR (300 MHz, CDCl_3 ; δ (ppm)): 10.3 (1H, s), 9.36 (1H, br s), 4.15 (2H, q, $J = 7.2$ Hz), 3.67 (2H, dt, $J = 6.9$ Hz), 2.40 (2H, t, $J = 7.2$ Hz), 1.99 (2H, qt, $J = 7.2$ Hz), 1.27 (3H, t, $J = 7.2$ Hz). ^{13}C NMR (75 MHz, CDCl_3 ; δ (ppm)): 190.7, 172.8, 166.3, 163.0, 162.1, 106.9, 60.9, 40.8, 31.6, 24.5, 14.4. HRMS (ESI, positive mode): m/z 306.0410 $[\text{M} + \text{H}]^+$ (calcd mass for $\text{C}_{11}\text{H}_{14}\text{Cl}_2\text{N}_3\text{O}_3$ $[\text{M} + \text{H}]^+$: 306.0412). Data for **4b** are as follows. TLC: R_f (20% AcOEt/hexane) 0.24. ^1H NMR (300 MHz, CDCl_3 ; δ (ppm)): 10.25 (1H, s), 6.27 (1H, br s), 4.15 (2H, q, $J = 7.2$ Hz), 3.59 (2H, dt, $J = 6.9$ Hz), 2.41 (2H, t, $J = 7.2$ Hz), 1.99 (2H, qt, $J = 7.2$ Hz), 1.27 (3H, t, $J = 7.2$ Hz). ^{13}C NMR (75 MHz, CDCl_3 ; δ (ppm)): 185.0, 173.1, 165.2, 163.9, 160.5, 114.4, 60.9, 41.5, 31.6, 24.4, 14.4; MS (ESI, positive mode): m/z 306.3 $[\text{M} + \text{H}]^+$ (calcd mass for $\text{C}_{11}\text{H}_{14}\text{Cl}_2\text{N}_3\text{O}_3$ $[\text{M} + \text{H}]^+$: 306.0412).

Ethyl 4-((2-Amino-6-chloro-5-formylpyrimidin-4-yl)amino)butanoate (5). To a stirred solution of **4a** (8.33 g, 27.3 mmol) in absolute ethanol (250 mL) were added 55 mL (819 mmol) of a 3/7 (v/v) mixture of 32% NH_4OH (w/w) and EtOH at room temperature. After it was stirred for 5 h at room temperature, the reaction mixture was evaporated to dryness. The residue was dissolved in AcOEt (100 mL) and the solution washed with water (2 \times 50 mL) and brine (50 mL). The organic phase was taken up, dried over anhydrous MgSO_4 , filtered, and concentrated in vacuo to dryness, providing the desired product as a yellow solid (7.84 g, quantitative yield), which was used without further purification in the next step. TLC: R_f (50% AcOEt/hexane) 0.57. ^1H NMR (400 MHz, CDCl_3 ; δ (ppm)): 10.08 (1H, s), 9.27 (1H, br s), 5.41 (2H, br s), 4.14 (2H, q, $J = 7.2$ Hz), 3.55 (2H, dt, $J = 6.9$ Hz), 2.38 (2H, t, $J = 7.2$ Hz), 1.95 (2H, qt, $J = 7.2$ Hz), 1.26 (3H, t, $J = 7.2$ Hz). ^{13}C NMR (100 MHz, CDCl_3 ; δ (ppm)): 188.9, 173.1, 166.7, 162.9, 162.4, 102.7, 60.7, 39.9, 31.7, 24.7, 14.3. HRMS (ESI, positive mode): m/z 287.0911 $[\text{M} + \text{H}]^+$ (calcd mass for $\text{C}_{11}\text{H}_{16}\text{ClN}_4\text{O}_3$ $[\text{M} + \text{H}]^+$: 287.0911).

Ethyl 4-((2-Amino-5-formylpyrimidin-4-yl)amino)butanoate (6). To a stirred solution of **5** (7.80 g, 27.21 mmol) and NaOAc (4.35 g, 108.8 mmol) in absolute EtOH (250 mL) was added 10% Pd/C (521 mg, 0.49 mmol) under an Ar atmosphere. The reaction mixture was stirred at room temperature under atmospheric pressure of H_2 for 15 h. On the basis of TLC analysis, additional 10% Pd/C (1 mmol) and NaOAc (54.42 mmol) were required for the reaction to reach completion within 6 h. The reaction mixture was filtered through Celite (previously washed with EtOH), and the product was eluted with EtOH (50 mL) and MeOH (4 \times 50 mL). The combined filtrates were collected together and evaporated in vacuo, affording a slightly yellow solid. After flash column chromatography (gradient AcOEt/hexane (1/1)–100% AcOEt–2% MeOH/AcOEt) the desired compound (**6**) was obtained as a white solid (3.87 g, 56%). TLC: R_f (AcOEt) 0.28. ^1H NMR (400 MHz, CDCl_3 ; δ (ppm)): 9.50 (1H, s), 8.63 (1H, br s), 8.15 (1H, s), 4.14 (2H, q, $J = 7.2$ Hz), 3.54 (2H, dt, $J = 6.8$ Hz), 2.39 (2H, t, $J = 7.2$ Hz), 1.96 (2H, qt, $J = 7.2$ Hz), 1.26 (3H, t, $J = 7.2$ Hz). ^{13}C NMR (100 MHz, CDCl_3 ; δ (ppm)): 189.2, 173.1, 166.1, 163.8, 161.8, 107.2, 60.6, 39.3, 31.8, 24.8, 14.4. HRMS (ESI, positive mode): m/z 253.1298 $[\text{M} + \text{H}]^+$ (calcd mass for $\text{C}_{11}\text{H}_{17}\text{N}_4\text{O}_3$ $[\text{M} + \text{H}]^+$: 253.1301).

Ethyl 4-((2-Bis(tert-butoxycarbonyl)amino-5-formylpyrimidin-4-yl)amino)butanoate (7). Compound **6** (3.87 g, 15.34 mmol) was dissolved in anhydrous DCM (100 mL) under Ar. Then, anhydrous triethylamine (10.2 mL, 67.5 mmol), DMAP (187 mg, 1.53 mmol), and Boc_2O (7.4 g, 33.75 mmol) were added sequentially. After it was stirred under Ar for 18 h, the reaction mixture was evaporated in vacuo. The residue was dissolved in AcOEt (100 mL) and the solution washed with 10% citric acid (50 mL), 10% NaHCO_3 (125 mL), and brine (50 mL). The organic phase was taken up, dried over anhydrous MgSO_4 , filtered, and concentrated in vacuo to dryness. After flash column chromatography (gradient 0–50% AcOEt in hexane), the

desired compound (**7**) was obtained as a white solid (4.1 g, 29.3%). TLC: R_f (AcOEt) 0.84. Mp: 163–173 °C. ^1H NMR (400 MHz, CDCl_3 ; δ (ppm)): 9.77 (1H, s), 8.65 (1H, br t), 8.52 (1H, s), 4.14 (2H, d, $J = 7.2$ Hz), 3.58 (2H, q, $J = 6.8$ Hz), 2.37 (2H, t, $J = 7.2$ Hz), 1.97 (2H, qt, $J = 7.2$ Hz), 1.53 (18H, s), 1.26 (3H, t, $J = 7.2$ Hz). ^{13}C NMR (100 MHz, CDCl_3 ; δ (ppm)): 190.8, 172.9, 165.3, 161.3, 160.3, 150.4, 110.3, 83.9, 60.7, 39.9, 31.7, 27.9, 24.6, 14.3. HRMS (ESI, positive mode): m/z 453.2352 $[\text{M} + \text{H}]^+$ (calcd mass for $\text{C}_{21}\text{H}_{33}\text{N}_4\text{O}_7$ $[\text{M} + \text{H}]^+$: 453.2349).

Ethyl 4-((2-Bis(tert-butoxycarbonyl)amino-5-((hydroxyimino)methyl)pyrimidin-4-yl)amino)butanoate (8). To a solution of compound **7** (4.22 g, 9.33 mmol) in pyridine (100 mL) was added hydroxylamine hydrochloride (1.3 g, 18.7 mmol), and the mixture was stirred under Ar for 6 h. The solvent was evaporated in vacuo, and after several coevaporations from toluene, the residue was dissolved in AcOEt (100 mL). The organic phase was washed with water (50 mL) and brine (50 mL), dried over anhydrous MgSO_4 , filtered, and concentrated in vacuo to dryness. The desired compound (**8**) was obtained as a yellow solid (3.85 g, 88%) and used in the next step without further purification. TLC: R_f (AcOEt) 0.84. IR (KBr): ν 3337.8, 1798.5, 1729.6, 1616.1, 1587.1 cm^{-1} . ^1H NMR (400 MHz, CDCl_3 ; δ (ppm)): 8.13 (1H, s), 8.13 (1H, s), 8.05 (1H, br s), 8.00 (1H, br s), 4.12 (2H, q, $J = 7.2$ Hz), 3.58 (2H, dt, $J = 6.8$ Hz), 2.37 (2H, t, $J = 7.2$ Hz), 1.96 (2H, qt, $J = 7.2$ Hz), 1.48 (18H, s), 1.24 (3H, t, $J = 7.2$ Hz). ^{13}C NMR (100 MHz, CDCl_3 ; δ (ppm)): 173.3, 160.1, 157.7, 157.2, 150.9, 147.9, 107.2, 83.2, 60.6, 40.1, 31.8, 28.0, 24.8, 14.3. HRMS (ESI, positive mode): m/z 468.2454 $[\text{M} + \text{H}]^+$ (calcd mass for $\text{C}_{21}\text{H}_{34}\text{N}_5\text{O}_7$ $[\text{M} + \text{H}]^+$: 468.2458).

Ethyl 4-((2-Bis(tert-butoxycarbonyl)amino-5-cyanopyrimidin-4-yl)amino)butanoate (9). To a solution of compound **8** (3.85 g, 8.24 mmol) in anhydrous THF (100 mL) was added triethylamine (3.7 mL, 24.72 mmol) under Ar. Then, the solution was cooled to 0 °C and trifluoroacetic anhydride (1.7 mL, 12.36 mmol) was added slowly with stirring. The mixture was warmed to room temperature and stirred for 2 h. The mixture was cooled to 0 °C, cold water (2 mL) was added to destroy the excess TFAA, and the solvent was evaporated in vacuo. The residue was dissolved in AcOEt (50 mL), and the solution was washed with 10% citric acid (25 mL), 10% NaHCO_3 (25 mL), and brine (25 mL). The organic phase was taken up, dried over anhydrous MgSO_4 , filtered, and evaporated in vacuo. The desired compound (**9**) was obtained after flash column chromatography (gradient 0–25% AcOEt in hexane) as a white solid (2.94 g, 79%). TLC: R_f (22.5% AcOEt in hexane) 0.44. Mp: 189–193 °C. IR (KBr): ν 3322.8, 2227.7, 1787.9, 1734.5, 1598, 1580.7 cm^{-1} . ^1H NMR (400 MHz, CDCl_3 ; δ (ppm)): 8.42 (1H, s), 6.12 (1H, br t, $J = 5.4$ Hz), 4.16 (2H, q, $J = 7.2$ Hz), 3.57 (2H, dt, $J = 6.8$ Hz), 2.40 (2H, t, $J = 7.2$ Hz), 1.97 (2H, qt, $J = 7.2$ Hz), 1.51 (18H, s), 1.27 (3H, t, $J = 7.2$ Hz). ^{13}C NMR (100 MHz, CDCl_3 ; δ (ppm)): 173.4, 162.4, 161.2, 159.6, 150.3, 114.9, 88.6, 84.1, 61.0, 41.0, 31.8, 29.9, 24.2, 14.4. HRMS (positive mode): m/z 450.2352 $[\text{M} + \text{H}]^+$ (calcd mass for $\text{C}_{21}\text{H}_{32}\text{N}_5\text{O}_6$ $[\text{M} + \text{H}]^+$: 450.2353).

Ethyl 4-((1-(2-Bis(tert-butoxycarbonyl)amino-5-cyanopyrimidin-4-yl)-3-(2,2,2-trichloroacetyl)ureido)butanoate (10). To a solution of compound **9** (1 g, 0.636 mmol) in anhydrous DCM (5 mL) was added a solution of trichloroacetyl isocyanate (0.78 mL, 6.36 mmol) in anhydrous DCM (9 mL) dropwise at 0 °C over a period of 10 min under an Ar atmosphere. After it was stirred for 1 h at 0 °C, the reaction mixture was warmed to room temperature and stirred for an additional 5 h. The reaction mixture was cooled to 0 °C and quenched with cold water (25 mL). The organic phase was taken up, washed with water (3 \times 15 mL), dried over anhydrous MgSO_4 , filtered, and evaporated in vacuo. The desired compound (**10**) was obtained after flash column chromatography (gradient 0–50% AcOEt in hexane) as a yellow solid (1.92 g, quantitative). TLC: R_f (AcOEt) 0.93. Mp: 134–137 °C. ^1H NMR (400 MHz, CDCl_3 ; δ (ppm)): 9.53 (1H, s), 4.32 (2H, $J = 6.8$ Hz), 4.12 (2H, q, $J = 7.2$ Hz), 2.41 (2H, t, $J = 7.2$ Hz), 2.10 (2H, qt, $J = 7.2$ Hz), 1.57 (18H, s), 1.24 (3H, t, $J = 7.2$ Hz). ^{13}C NMR (100 MHz, CDCl_3 ; δ (ppm)): 174.0, 172.7, 163.9, 160.8, 159.1, 158.2, 149.5, 147.5, 104.6, 92.0, 85.1, 60.8, 42.1, 31.6, 27.9, 22.9, 14.3.

HRMS (ESI, positive mode): m/z 637.1336 $[M + H]^+$ (calcd mass for $C_{24}H_{32}Cl_3N_6O_8$ $[M + H]^+$: 637.1342).

Ethyl 4-(4-Amino-7-(bis(tert-butoxycarbonyl)amino)-2-oxopyrimido[4,5-d]pyrimidin-1(2H)-yl)butanoate (11). Compound **10** (1.42 g, 2.23 mmol) was stirred in 7 N NH_3 in MeOH (50 mL) under an Ar atmosphere at -10 °C (ice–NaCl bath) for 2 h. After evaporation in vacuo, the resulting solid was dissolved in DCM (30 mL). The organic phase was washed with water (3×25 mL), dried over anhydrous $MgSO_4$, filtered, and evaporated in vacuo. The desired compound (**11**) was obtained as a yellow solid (878 mg, 80.1%) and used without further purification in the next step. TLC: R_f (15% MeOH/AcOEt) 0.68. IR (NaCl): ν 3400, 1738.8, 1652.6, 1635.5, 1602.3, 1558.9, 1540 cm^{-1} . 1H NMR (400 MHz, $CDCl_3$; δ (ppm)): 9.28 (1H, s), 4.27 (2H, t, $J = 7.2$ Hz), 4.10 (2H, q, $J = 7.2$ Hz), 2.38 (2H, t, $J = 7.6$ Hz), 2.05 (2H, qt, $J = 7.6$ Hz), 1.53 (18H, s), 1.22 (3H, t, $J = 7.2$ Hz). ^{13}C NMR (100 MHz, $CDCl_3$; δ (ppm)): 173.0, 161.4, 160.4, 158.7, 156.8, 155.9, 150.2, 101.1, 84.5, 60.6, 41.4, 31.8, 27.9, 23.3, 14.3. HRMS (ESI, positive mode): m/z 493.2411 $[M + H]^+$ (calcd mass for $C_{22}H_{33}N_6O_7$ $[M + H]^+$: 493.2405).

Ethyl 4-(7-(Bis(tert-butoxycarbonyl)amino)-4-((tert-butoxycarbonyl)amino)-2-oxopyrimido[4,5-d]pyrimidin-1(2H)-yl)butanoate (12). To a solution of compound **11** (878 mg, 2.23 mmol) in anhydrous DCM (30 mL) were added anhydrous triethylamine (1.62 mL, 13.38 mmol), DMAP (218 mg, 2.23 mmol), and Boc_2O (1.17 g, 6.69 mmol) under an Ar atmosphere. After the mixture was stirred for 24 h at room temperature, the color changed from yellow to brown. The reaction mixture was taken up and the organic phase was washed with water (2×25 mL) 10% citric acid (25 mL), 10% $NaHCO_3$ (25 mL), and brine (25 mL) and then dried over anhydrous $MgSO_4$ and filtered. After removal of the solvent under reduced pressure, compound **12** was obtained as a brown solid (1.11 g, 90%), which was used without further purification in the next step. TLC: R_f (50% AcOEt/hexane) 0.78. 1H NMR (400 MHz, $CDCl_3$; δ (ppm)): 9.42 (1H, s), 4.24 (2H, t, $J = 7.2$ Hz), 4.09 (2H, q, $J = 7.2$ Hz), 2.37 (2H, t, $J = 7.2$ Hz), 2.04 (2H, qt, $J = 7.2$ Hz), 1.54 (18H, s), 1.50 (9H, s), 1.22 (3H, t, $J = 7.2$ Hz). ^{13}C NMR (100 MHz, $CDCl_3$; δ (ppm)): 172.6, 161.2, 159.3, 158.0, 157.9, 155.6, 149.9, 148.2, 105.6, 84.9, 84.5, 60.7, 41.5, 31.6, 28.1, 27.9, 23.1, 14.3. HRMS (ESI, positive mode): m/z 593.2937 $[M + H]^+$ (calcd mass for $C_{27}H_{41}N_6O_9$ $[M + H]^+$: 593.2930).

4-(7-(Bis(tert-butoxycarbonyl)amino)-4-((tert-butoxycarbonyl)amino)-2-oxopyrimido[4,5-d]pyrimidin-1(2H)-yl)butanoic Acid (1). To a solution of **12** (550 mg, 0.325 mmol) in a 3/1 (v/v) mixture of H_2O and ACN (30 mL) was added a solution of LiOH (400 mg, 3.25 mmol) in water (1 mL). After it was stirred for 1 h at room temperature, the reaction mixture was concentrated in vacuo to remove ACN. The resulting aqueous phase was acidified with 10% citric acid to pH 3–4, causing the precipitation of a white solid, which was redissolved in AcOEt (10 mL). The organic phase was taken up, and the aqueous phase was washed with AcOEt (2×10 mL). The combined organic phases were dried over anhydrous $MgSO_4$, filtered, and evaporated in vacuo. The desired compound (**1**) was obtained after flash column chromatography (gradient 50–100% AcOEt in hexane, 100% AcOEt–15% MeOH in AcOEt) as a yellow solid (130 mg, 27.3%). TLC: R_f (AcOEt) 0.80. Mp: 190–193 °C. IR (KBr): ν 3362.5, 1764.3, 1751.3, 1728.6, 1661.5, 1602.3 cm^{-1} . 1H NMR (400 MHz, $CDCl_3$; δ (ppm)): 12.10 (1H, br s), 9.43 (1H, s), 4.28 (2H, t, $J = 6.8$ Hz), 2.44 (2H, t, $J = 7.2$ Hz), 2.07 (2H, qt, $J = 7.2$ Hz), 1.57 (9H, s), 1.51 (18H, s). ^{13}C NMR (100 MHz, $CDCl_3$; δ (ppm)): 177.4, 162.6, 161.2, 159.3, 158.0, 155.5, 149.9, 148.1, 105.6, 84.6, 82.1, 41.3, 31.1, 28.1, 27.9, 22.9. HRMS (ESI, positive mode): m/z 565.2618 $[M + H]^+$ (calcd mass for $C_{25}H_{37}N_6O_9$ $[M + H]^+$: 565.2617).

Synthesis of Janus B Monomer (2). **5-(4,6-Diamino-1,3,5-triazin-2-yl)cytosine (15).** To a suspension of compound **14** (5 g, 36.8 mmol) in ethylene glycol (100 mL) was added a solution of KOH (4.1 g, 73.5 mmol) and dicyandiamide (6.18 g, 73.5 mmol) in ethylene glycol (100 mL) dropwise under an Ar atmosphere over a period of 10 min. The resulting red-brown solution was refluxed at 150 °C for 40 h. After evaporation in vacuo, the resulting brown solid was washed with water, diethyl ether, and EtOH. Finally, compound **15** was obtained as

a brown solid (4.53 g, 54%) and used without further purification in the next step. 1H NMR (400 MHz, DMSO; δ (ppm)): 9.46 (1H, br s), 8.51 (1H, s), 8.01 (1H, br s), 6.81 (5H, br s). ^{13}C NMR (100 MHz, DMSO; δ (ppm)): 167.9, 165.9, 164.2, 156.0, 148.6, 99.2. HRMS (ESI, positive mode): m/z 221.0893 $[M + H]^+$ (calcd mass for $C_7H_9N_8O$ $[M + H]^+$: 221.0899).

4-(5-(4,6-Diamino-1,3,5-triazin-2-yl)cytosine-1(2H)-yl)butanoic Acid (2). To a solution of compound **15** (630 mg, 2.86 mmol) in anhydrous DMF was added NaH 60% dispersion in mineral oil (114.4 mg, 2.86 mmol) under an Ar atmosphere, and the reaction mixture was stirred at 50 °C for 2 h. Then, ethyl bromobutyrate (450 μ L, 3.15 mmol) was slowly added dropwise, and the mixture was stirred at room temperature for 15 h. After evaporation in vacuo, the residue was dissolved in 30% MeOH in H_2O (200 mL) at 70 °C and then warmed to room temperature. The precipitate was removed by filtration and identified as the starting compound (**15**). The filtrate was evaporated in vacuo, affording a solid that contained ethyl 4-(5-(4,6-diamino-1,3,5-triazin-2-yl)cytosine-1(2H)-yl)butanoate (**16**) as the major component (80%) according to HPLC-MS analysis. The crude product, which was not purified further due to its poor solubility in organic solvents, was dissolved in aqueous 1 M LiOH (100 mL), and the brown solution was stirred overnight at room temperature. Then, 10% HCl was added until pH 2. After evaporation in vacuo, purification was accomplished by MPLC with a gradient from 0 to 100% of B as eluent (A, 0.1% formic acid in H_2O ; B, 0.1% formic acid in H_2O /ACN 1/1; 1 L each solvent). Pure fractions by MS-HPLC (linear gradient from 0 to 100% B in 18 min; A, 0.1% formic acid in H_2O ; B, 0.1% formic acid in ACN; $R_t = 7.2$ min) were combined and lyophilized, providing the desired product (**2**) as a yellow solid (143 mg, 20%). Data for **16** are as follows. MS-HPLC (0 a 100% B in 18 min): $R_t = 3.5$ min. MS (ESI, positive mode): m/z 335.04 $[M + H]^+$ (calcd mass for $C_{13}H_{19}N_8O_3$ $[M + H]^+$: 335.1580). Data for **2** are as follows. HPLC (0 a 50% B in 30 min): $R_t = 14.6$ min. 1H NMR (500 MHz, DMSO; δ (ppm)): 12.21 (1H, br s), 10.74 (1H, br s), 9.10 (1H, br s), 8.79 (1H, s), 7.06 (4H, br s), 3.91 (2H, t, $J = 7.0$ Hz), 2.32 (2H, t, $J = 7.0$ Hz), 1.88 (2H, t, $J = 7.0$ Hz). ^{13}C NMR (100 MHz, DMSO; δ (ppm)): 173.9, 167.7, 166.0, 163.9, 154.4, 149.6, 100.3, 49.0, 30.7, 24.4. HRMS (ESI, positive mode): m/z 307.1261 $[M + H]^+$ (calcd mass for $C_{11}H_{13}N_8O_3$ $[M + H]^+$: 307.1267).

Solid-Phase Synthesis of Janus-Peptide Derivatives (18 and 19). **Fmoc-Asn(Trt)-Arg(Pbf)-Cys(Trt)-resin (17).** The peptide was synthesized on a Rink amide *p*-MBHA resin ($f = 0.74$ mmol/g, 100–200 mesh) using standard Fmoc/tBu chemistry with Fmoc-protected amino acids (4 mol equiv), DIPC (4 mol equiv), and HOAt (4 mol equiv) for the coupling (2 h, DMF). The following side chain protecting groups were used: Trt (*N*-Trityl, asparagine; *S*-Trityl, cysteine), and Pbf (*N*^G-2,2,4,6,7-pentamethylidihydrobenzofuran-5-sulfonyl, arginine).

4-(4,7-Diamino-2-oxopyrimido[4,5-d]pyrimidin-1(2H)-yl)-*N*-[Asn-Arg-Cys-NH₂]butanamide (18). Peptide-bound resin **17** (60 mg, 0.044 mmol, $f \approx 0.74$ mmol/g) was introduced into a polypropylene syringe fitted with a polyethylene disk, treated with 20% piperidine in DMF (2×10 min), washed successively (30 s washes) with DMF, DCM, and MeOH, and dried directly on a vacuum filtration system. Janus A monomer **1** (33 mg, 0.059 mmol) was activated with HATU (20.3 mg, 0.053 mmol) and DIPEA (19 μ L, 0.111 mmol) in the minimum amount of anhydrous DMF for 2 min, and the resulting yellow solution was added to the solid support, which was occasionally stirred with a Teflon rod for 4 h at room temperature. After vacuum filtration and washings ($3 \times$ DMF, $3 \times$ DCM, and $3 \times$ MeOH), side chain deprotection and cleavage from the resin was performed simultaneously with TFA/TIS/ H_2O 95/2.5/2.5 (1 mL) for 1 h at room temperature. Most of the TFA was removed by bubbling N_2 into the solution, and the resulting residue was poured onto cold ether to precipitate the target compound. Analytical HPLC (linear gradient from 0 to 35% B in 30 min; A, 0.045% TFA in H_2O ; B, 0.036% TFA in ACN) revealed the presence of a main peak ($R_t = 13.1$ min, 73%), which was characterized as the desired compound **18**. HRMS (ESI, positive mode): m/z 637.2744 $[M + H]^+$ (calcd mass for $C_{23}H_{37}N_{14}O_6S$ $[M + H]^+$: 637.2736).

4-(5-(4,6-Diamino-1,3,5-triazin-2-yl)cytosin-1(2H)-yl)-N-[Asn-Arg-Cys-NH₂]butanamide (**19**). Peptide-bound resin **17** (34 mg, 0.025 mmol, $f \approx 0.74$ mmol/g) was introduced into a polypropylene syringe fitted with a polyethylene disk, treated with 20% piperidine in DMF (2 × 10 min), washed successively (30 s washes) with DMF, DCM, and MeOH, and dried directly on a vacuum filtration system. Janus B monomer **2** (10 mg, 0.032 mmol) was activated with HATU (11.5 mg, 0.030 mmol) and DIPEA (11 μL, 0.629 mmol) in the minimum amount of anhydrous DMF for 2 min, and the resulting yellow solution was added to the solid support, which was occasionally stirred with a Teflon rod for 4 h at room temperature. After vacuum filtration and washings (3 × DMF, 3 × DCM, and 3 × MeOH), side chain deprotection and cleavage from the resin was performed with TFA/TIS/H₂O 95/2.5/2.5 (1 mL) for 1 h at room temperature. Most of the TFA was removed by bubbling N₂ into the solution, and the resulting residue was poured onto cold ether to precipitate the target compound. Analytical HPLC (linear gradient from 0 to 35% B in 30 min; A, 0.045% TFA in H₂O; B, 0.036% TFA in ACN) revealed the presence of a main peak ($R_t = 14.1$ min, 54%), which was characterized as the desired compound **19**. HRMS (ESI, positive mode): m/z 679.2953 [M + H]⁺ (calcd mass for C₂₄H₃₉N₁₆O₆S [M + H]⁺: 679.2954).

Synthesis of Janus-Neamine Ligands (20–23). General Procedure. To a solution of 2,2'-dithiobis(5-nitropyridine) (7.8 mg, 25 μmol) in THF (2 mL) was added under argon a solution of the neamine thiol derivative (Nea or Nea2, 2 μmol)¹¹ in aqueous 0.1% TFA (1 mL), and the mixture was stirred at room temperature. After 15 h, THF was evaporated in vacuo and the remaining yellow solution was diluted with H₂O (2 mL). The aqueous phase was washed with AcOEt to remove the excess 2,2'-dithiobis(5-nitropyridine) (typically 5 × 2 mL or until no yellow color was detected in the organic phase), lyophilized, and dissolved again in aqueous 0.1% TFA (1 mL) under argon. Then, a solution of **18** or **19** (2 μmol) in 0.1% TFA/H₂O (1 mL) was added over the activated Janus-containing solution, and the mixture was stirred overnight under argon at room temperature. After purification by semipreparative reversed-phase HPLC (linear gradient from 0 to 35% B in 35 min; A, 0.1% TFA in H₂O; B, 0.036% TFA in ACN) and lyophilization, the TFA salt of the desired product was obtained as a white solid.

JanusA-Nea (20). Yield: 33%. ¹H NMR (600 MHz, D₂O; δ (ppm)): 8.82 (1H, H_{Ar}, s), 5.45 (1H, H_{1'}, m), 4.63–4.61 (2H, H_{α1}, H_{α3}, m), 4.35 (1H, H_{α2}, m), 4.17 (2H, -NCH₂-, m), 3.99 (1H, H₅, m), 3.91 (1H, -OCH₂-, m), 3.76 (1H, -OCH₂-, m), 3.65 (1H, H₆, m), 3.49 (2H, H₄, H₅, m), 3.40 (3H, H₂, H₃, H₄, m), 3.19 (5H, H₆, H_{δ2}, H_{β3}, m), 2.94 (1H, H_{β3}, m), 2.83 (1H, H_{β1}, m), 2.78 (1H, H_{β1}, m), 2.67 (2H, -SCH₂-, m), 2.40 (2H, -CH₂CO-, m), 2.16 (2H, H₁, H₃, m), 1.99 (2H, -NCH₂CH₂-, m), 1.92 (1H, H_{β2}, m), 1.81 (1H, H_{β2}, m), 1.61 (7H, H_{2,eq}, H_{7,2}, -OCH₂CH₂-, SCH₂CH₂-, m), 1.33 (5H, H_{2,ax}, -OCH₂CH₂CH₂CH₂-, m). HRMS (ESI, positive mode): m/z 1073.5088 [M + H]⁺ (calcd mass for C₄₁H₇₃N₁₈O₁₂S₂ [M + H]⁺: 1073.5097). Analytical reversed-phase HPLC (0 to 35% B in 35 min): $R_t = 17.8$ min.

JanusA-Nea2 (21). Yield: 21%. ¹H NMR (600 MHz, D₂O; δ (ppm)): 8.77 (1H, H_{Ar}, s), 5.81 (1H, H_{1'}, d, $J = 3.8$ Hz), 4.61 (1H, H_{α3}, m), 4.56 (1H, H_{α1}, t, $J = 7.0$ Hz), 4.29 (1H, H_{α2}, m), 4.18 (1H, -OCH₂-, m), 4.07 (2H, -NCH₂-, m), 3.92 (2H, H₅, -OCH₂-, m), 3.68 (1H, H₆, m), 3.49 (2H, H₆, m), 3.41 (3H, H₄, H₄, H₃, m), 3.29 (2H, H₂, H₅, m), 3.17 (1H, H_{β3}, m), 3.06 (2H, H_{δ2}, m), 2.91 (3H, -SCH₂-, H_{β3}, m), 2.77 (1H, H_{β1}, m), 2.67 (1H, H_{β1}, m), 2.38 (2H, H₁, H₃, m), 2.33 (2H, -CH₂CO-, m), 1.91 (2H, -NCH₂CH₂-, m), 1.88 (1H, H_{β2}, m), 1.73 (2H, H_{β2}, H_{2,eq}, m), 1.55 (3H, H_{7,2}, H_{2,ax}, m). HRMS (ESI, positive mode): m/z 1017.4431 [M + H]⁺ (calcd mass for C₃₇H₆₅N₁₈O₁₂S₂ [M + H]⁺: 1017.4471). Analytical reversed-phase HPLC (0 to 35% B in 30 min): $R_t = 13.3$ min.

JanusB-Nea (22). Yield: 21%. ¹H NMR (600 MHz, D₂O; δ (ppm)): 8.72 (1H, H_{Ar}, s), 5.67 (1H, H_{1'}, m), 4.61 (1H, H_{α3}, m), 4.58 (1H, H_{α1}, t, $J = 6.9$ Hz), 4.34 (1H, H_{α2}, m), 3.96 (1H, -OCH₂-, m), 3.88 (3H, -NCH₂-, H₅, m), 3.75 (1H, -OCH₂-, m), 3.63 (2H, H₄, H₆, m), 3.60 (1H, H₃, m), 3.45 (3H, H₂, H₄, H₅, m), 3.25 (2H, H₆, m), 3.19 (3H, H_{δ2}, H_{β3}, m), 2.94 (1H, H_{β3}, m), 2.80 (1H, H_{β1}, m),

2.76 (1H, H_{β1}, m), 2.67 (2H, -SCH₂-, m), 2.40 (2H, -CH₂CO-, t, $J = 7.4$ Hz), 2.27 (2H, H₁, H₃, m), 2.06 (2H, -NCH₂CH₂-, m), 1.89 (1H, H_{β2}, m), 1.80 (1H, H_{β2}, m), 1.60 (7H, -SCH₂CH₂-, -OCH₂CH₂-, H_{2,eq}, H_{7,2}, m), 1.32 (5H, H_{2,ax}, -OCH₂CH₂CH₂CH₂-, m). HRMS (ESI, positive mode): m/z 1115.5302 [M + H]⁺ (calcd mass for C₄₂H₇₅N₂₀O₁₂S₂ [M + H]⁺: 1115.5315). Analytical reversed-phase HPLC (0 to 35% B in 35 min): $R_t = 18.5$ min.

JanusB-Nea2 (23). Yield: 53%. ¹H NMR (600 MHz, D₂O; δ (ppm)): 8.70 (1H, H_{Ar}, s), 5.70 (1H, H_{1'}, m), 4.66 (1H, H_{α3}, m), 4.60 (1H, H_{α1}, t, $J = 6.9$ Hz), 4.34 (1H, H_{α2}, m), 4.18 (1H, -OCH₂-, m), 3.99 (2H, H₅, -OCH₂-, m), 3.94 (2H, -NCH₂-, m), 3.65 (2H, H₄, H₆, m), 3.46 (3H, H₅, H₃, H₄, m), 3.25 (4H, H₂, H₆, H_{β3}, m), 3.17 (2H, H_{δ2}, t, $J = 7.3$ Hz), 2.99 (3H, -SCH₂-, H_{β3}, m), 2.81 (1H, H_{β1}, m), 2.73 (1H, H_{β1}, m), 2.41 (2H, -CH₂CO-, t, $J = 7.2$ Hz), 2.25 (2H, H₁, H₃, m), 2.07 (2H, -NCH₂CH₂-, m), 1.91 (1H, H_{β2}, m), 1.79 (2H, H_{2,eq}, H_{β2}, m), 1.60 (3H, H_{2,ax}, H_{7,2}, m). HRMS (ESI, positive mode): m/z 1059.4675 [M + H]⁺ (calcd mass for C₃₈H₆₇N₂₀O₁₂S₂ [M + H]⁺: 1059.4689). Analytical reversed-phase HPLC (0 to 35% B in 30 min): $R_t = 14.8$ min.

Synthesis of Janus-Guanidinoneamine Ligands (24–27). General Procedure. The Janus-neamine ligand (**20–23**, 300 nmol) and 1,3-di-Boc-2-trifluoromethylsulfonylguanidine (4.7 mg, 12 μmol) were dissolved in a 5/3 (v/v) mixture of MeOH and CHCl₃ (0.5 mL) under an argon atmosphere. Then, triethylamine (10 μL, 72 μmol) was added and the reaction mixture was stirred for 4 days at room temperature under Ar. After evaporation in vacuo, the crude product was diluted with DCM (5 mL) and washed with a 10% aqueous solution of citric acid (3 × 1 mL) and with brine (3 × 1 mL). The organic phase was taken up and dried over anhydrous MgSO₄, filtered, and concentrated in vacuo to dryness. The crude product was dissolved in a 1/1 (v/v) mixture of TFA and DCM (0.5 mL), and TIS (12.5 μL, 61 μmol) was added. After it was stirred at room temperature for 2 h under Ar, the mixture was diluted with toluene (2 mL) and evaporated in vacuo. After several coevaporations from toluene, the residue was dissolved in Milli-Q H₂O (5 mL) and lyophilized to provide a white solid. Purification was carried out by analytical reversed-phase HPLC (linear gradient from 0 to 25% B in 35 min; A, 0.045% TFA in H₂O; B, 0.036% TFA in ACN), and the TFA salt of the desired product was obtained after lyophilization.

JanusA-NeaG4 (24). Yield: 24%. ¹H NMR (600 MHz, D₂O; δ (ppm)): 8.81 (1H, H_{Ar}, s), 5.59 (1H, H_{1'}, d, $J = 4.0$ Hz), 4.61 (2H, H_{α1}, H_{α3}, m), 4.35 (1H, H_{α2}, m), 4.13 (2H, -NCH₂-, m), 3.98 (1H, -OCH₂-, m), 3.72–3.45 (10H, -OCH₂-, H₂, H₃, H₄, H₅, H₆, H₄, H₅, H₆, m), 3.20 (1H, H_{β3}, m), 3.16 (2H, H_{δ2}, m), 2.92 (1H, H_{β3}, m), 2.81 (1H, H_{β1}, m), 2.76 (1H, H_{β1}, m), 2.66 (2H, -SCH₂-, m), 2.41 (2H, -CH₂CO-, m), 2.25 (2H, H₁, H₃, m), 1.98 (2H, -NCH₂CH₂-, m), 1.90 (1H, H_{β2}, m), 1.81 (1H, H_{β2}, m), 1.59 (5H, H_{2,eq}, H_{7,2}, -SCH₂CH₂-, m), 1.50 (2H, -OCH₂CH₂-, m), 1.36–1.23 (5H, H_{2,ax}, -OCH₂CH₂CH₂CH₂-, m). HRMS (ESI, positive mode): m/z 621.3023 [M + 2H]²⁺ (calcd mass for C₄₅H₈₂N₂₆O₁₂S₂ [M + 2H]²⁺: 621.3024), m/z 414.5366 [M + 3H]³⁺ (calcd mass for C₄₅H₈₃N₂₆O₁₂S₂ [M + 3H]³⁺: 414.5375), m/z 311.1542 [M + 4H]⁴⁺ (calcd mass for C₄₅H₈₄N₂₆O₁₂S₂ [M + H]⁺: 311.1551). Analytical reversed-phase HPLC (0 to 25% B in 35 min): $R_t = 23.4$ min.

JanusA-Nea2G4 (25). Yield: 24%. ¹H NMR (600 MHz, D₂O; δ (ppm)): 8.81 (1H, H_{Ar}, s), 5.66 (1H, H_{1'}, d, $J = 4.0$ Hz), 4.65 (1H, H_{α3}, m), 4.62 (1H, H_{α1}, t, $J = 7.0$ Hz), 4.35 (1H, H_{α2}, m), 4.21 (1H, -OCH₂-, m), 4.12 (2H, -NCH₂-, m), 3.81 (1H, -OCH₂-, m), 3.73 (2H, H₅, H₆, m), 3.63 (1H, H₂, m), 3.56 (4H, H₃, H₄, H₄, H₅, m), 3.47 (2H, H₆, m), 3.23 (1H, H_{β3}, m), 3.14 (2H, H_{δ2}, m), 2.92 (3H, -SCH₂-, H_{β3}, m), 2.81 (1H, H_{β1}, m), 2.75 (1H, H_{β1}, m), 2.40 (2H, -CH₂CO-, m), 2.23 (2H, H₁, H₃, m), 1.98 (2H, -NCH₂CH₂-, m), 1.90 (1H, H_{β2}, m), 1.79 (2H, H_{β2}, H_{2,eq}, m), 1.62 (3H, H_{7,2}, H_{2,ax}, m). HRMS (ESI, positive mode): m/z 593.2696 [M + 2H]²⁺ (calcd mass for C₄₁H₇₄N₂₆O₁₂S₂ [M + 2H]²⁺: 593.2711), m/z 395.8489 [M + 3H]³⁺ (calcd mass for C₄₁H₇₅N₂₆O₁₂S₂ [M + 3H]³⁺: 395.8500), m/z 297.1388 [M + 4H]⁴⁺ (calcd mass for C₄₁H₇₆N₂₆O₁₂S₂ [M + 4H]⁴⁺: 297.1394). Analytical reversed-phase HPLC (0 to 25% B in 35 min): $R_t = 17.8$ min.

JanusB-NeaG4 (26). Yield: 25%. ^1H NMR (600 MHz, D_2O ; δ (ppm)): 8.73 (1H, H_{Ar} , s), 5.59 (1H, $\text{H}_{1'}$, d, $J = 4.0$ Hz), 4.61 (1H, $\text{H}_{\alpha 3}$, m), 4.58 (1H, $\text{H}_{\alpha 1'}$, t, $J = 6.9$ Hz), 4.34 (1H, $\text{H}_{\alpha 2'}$, m), 3.98 (1H, $-\text{OCH}_2-$, m), 3.91 (2H, $-\text{NCH}_2-$, m), 3.70–3.45 (10H, $-\text{OCH}_2-$, H_2 , H_3 , H_4 , H_5 , H_6 , H_4 , H_5 , H_6 , m), 3.18 (3H, $\text{H}_{\beta 2'}$, $\text{H}_{\beta 3}$, m), 2.94 (1H, $\text{H}_{\beta 3}$, m), 2.80 (1H, $\text{H}_{\beta 1'}$, m), 2.74 (1H, $\text{H}_{\beta 1'}$, m), 2.66 (2H, $-\text{SCH}_2-$, m), 2.42 (2H, $-\text{CH}_2\text{CO}-$, t, $J = 7.3$ Hz), 2.25 (2H, H_1 , H_3 , m), 2.07 (2H, $-\text{NCH}_2\text{CH}_2-$, m), 1.90 (1H, $\text{H}_{\beta 2'}$, m), 1.82 (1H, $\text{H}_{\beta 2'}$, m), 1.59 (5H, SCH_2CH_2- , $\text{H}_{2,\text{eq}}$, $\text{H}_{2,\text{ax}}$, m), 1.49 (2H, $-\text{OCH}_2\text{CH}_2-$, m), 1.32–1.25 (5H, $\text{H}_{2,\text{ax}}$, $-\text{OCH}_2\text{CH}_2\text{CH}_2\text{CH}_2-$, m). HRMS (ESI, positive mode): m/z 642.3114 [$\text{M} + 2\text{H}$] $^{2+}$ (calcd mass for $\text{C}_{46}\text{H}_{84}\text{N}_{28}\text{O}_{12}\text{S}_2$ [$\text{M} + 2\text{H}$] $^{2+}$: 642.3132), m/z 428.5420 [$\text{M} + 3\text{H}$] $^{3+}$ (calcd mass for $\text{C}_{46}\text{H}_{85}\text{N}_{28}\text{O}_{12}\text{S}_2$ [$\text{M} + 3\text{H}$] $^{3+}$: 428.5448), m/z 321.6584 [$\text{M} + 4\text{H}$] $^{4+}$ (calcd mass for $\text{C}_{46}\text{H}_{86}\text{N}_{28}\text{O}_{12}\text{S}_2$ [$\text{M} + 4\text{H}$] $^{4+}$: 321.6605). Analytical reversed-phase HPLC (0 to 25% B in 35 min): $R_t = 24.1$ min.

JanusB-NeaG4 (27). Yield: 23%. ^1H NMR (600 MHz, D_2O ; δ (ppm)): 8.71 (1H, H_{Ar} , s), 5.65 (1H, $\text{H}_{1'}$, d, $J = 4.0$ Hz), 4.65 (1H, $\text{H}_{\alpha 3}$, m), 4.60 (1H, $\text{H}_{\alpha 1'}$, t, $J = 7.0$ Hz), 4.34 (1H, $\text{H}_{\alpha 2'}$, m), 4.21 (1H, $-\text{OCH}_2-$, m), 3.93 (2H, $-\text{NCH}_2-$, m), 3.82 (1H, $-\text{OCH}_2-$, m), 3.71 (3H, H_2 , H_3 , H_6 , m), 3.55 (4H, H_4 , H_5 , H_3 , H_4 , m), 3.48 (2H, H_6 , m), 3.25 (1H, $\text{H}_{\beta 3}$, m), 3.17 (2H, $\text{H}_{\beta 2'}$, m), 2.96 (3H, $-\text{SCH}_2-$, $\text{H}_{\beta 3}$, m), 2.81 (1H, $\text{H}_{\beta 1'}$, m), 2.72 (1H, $\text{H}_{\beta 1'}$, m), 2.41 (2H, $-\text{CH}_2\text{CO}$, t, $J = 7.2$ Hz), 2.24 (2H, H_1 , H_3 , m), 2.07 (2H, $-\text{NCH}_2\text{CH}_2-$, m), 1.90 (1H, $\text{H}_{\beta 2'}$, m), 1.79 (2H, $\text{H}_{2,\text{eq}}$, $\text{H}_{2,\text{ax}}$, m), 1.62 (3H, $\text{H}_{2,\text{ax}}$, $\text{H}_{2,\text{ax}}$, m). HRMS (ESI, positive mode): m/z 614.2806 [$\text{M} + 2\text{H}$] $^{2+}$ (calcd mass for $\text{C}_{42}\text{H}_{76}\text{N}_{28}\text{O}_{12}\text{S}_2$ [$\text{M} + 2\text{H}$] $^{2+}$: 614.2819), m/z 409.8561 [$\text{M} + 3\text{H}$] $^{3+}$ (calcd mass for $\text{C}_{42}\text{H}_{77}\text{N}_{28}\text{O}_{12}\text{S}_2$ [$\text{M} + 3\text{H}$] $^{3+}$: 409.8572), m/z 307.6442 [$\text{M} + 4\text{H}$] $^{4+}$ (calcd mass for $\text{C}_{42}\text{H}_{78}\text{N}_{28}\text{O}_{12}\text{S}_2$ [$\text{M} + 4\text{H}$] $^{4+}$: 307.6449). Analytical reversed-phase HPLC (0 to 25% B in 35 min): $R_t = 19.2$ min.

Evaluation of the Interaction between Tau RNA and Janus-Containing Ligands. Oligoribonucleotides were synthesized using 2'-*O*-*tert*-butyldimethylsilyl (TBDMS) protection and following standard procedures (phosphite triester approach). RNA, fluorescein, 2-AP phosphoramidites, solid supports, reagents, and solvents for oligoribonucleotide synthesis were purchased from Glen Research or Link Technologies. The syntheses (1 μmol scale) were performed on an ABI 3400 DNA automatic synthesizer according to the manufacturer's synthesis procedure, with some modifications.^{11a} Cleavage and deprotection from the solid support were carried out following a stepwise protocol.^{11a,28} RNase-free reagents, solutions, and materials were used when manipulating deprotected oligoribonucleotides. RNase-free water was obtained directly from a Milli-Q system equipped with a 5000 Da ultrafiltration cartridge. Reversed-phase high-performance liquid chromatography (HPLC) was used for both the analysis and purification of oligoribonucleotides using linear gradients of 0.1 M aqueous NH_4HCO_3 and a 1/1 mixture of 0.1 M aqueous NH_4HCO_3 and ACN. Characterization was carried out by high-resolution MALDI-TOF mass spectrometry (negative mode, 2,4,6-trihydroxyacetophenone matrix with ammonium citrate as an additive).

The following oligoribonucleotide sequences were synthesized (an asterisk label denotes that the ends of the chains were modified with 2'-*O*-methylribonucleosides): wt RNA, 5'rG*C*GGCAGUGUGAGUACCUUCACACGUCC*C*; +3 mutated RNA, 5'rG*C*GGCAGUGUGAGUACCUUCACACGUCC*C*; +16 mutated RNA, 5'rG*C*GGCAGUGUGAGUACCUUCACAUGUCC*C*. In fluorescence binding assays, fluorescein was attached at the 5'-end of wt RNA, and the adenine in the loop of the +3 mutated RNA sequence was replaced by 2-AP. NMR titration experiments were carried out with a shorter wt RNA sequence: 5'rGGCAGUGUGAGUACCUUCACACGUCC.

UV-Monitored Melting Experiments. Melting curves were recorded by cooling the samples from 90 to 20 $^\circ\text{C}$ at a constant rate of 0.5 $^\circ\text{C}$ min^{-1} and measuring the absorbance at 260 nm as a function of temperature. Then, the reverse denaturation curve (20 to 90 $^\circ\text{C}$) was recorded. All experiments were repeated at least three times until coincident T_m values were obtained. The error in T_m values was ± 0.2 $^\circ\text{C}$. The solutions were 1 μM both in RNA (wt, +3 or +16) and in

ligands, in 10 mM pH 6.8 sodium phosphate buffer, 50 mM NaCl, and 0.1 mM Na_2EDTA .

Fluorescence Binding Assays. Fluorescence measurements were performed in 1 cm path length quartz cells on a Quanta-Master fluorometer (PTI) at 25 $^\circ\text{C}$, with an excitation slit width of 10 nm and an emission slit width of 10 nm. Upon excitation at 290 nm, the emission spectrum was recorded over a range between 340 and 410 nm until no changes in the fluorescence intensity were detected. All binding assays were performed in the melting curves buffer with continuous magnetic stirring, except during the measurement.

For each experiment, the fluorescence spectrum of a 600 μL buffer solution without RNA or ligand was first taken, to be used as the baseline. Following this buffer blank, the spectrum of a 83 nM solution of refolded RNA containing 2-AP (600 μL) was recorded, and the baseline blank was subtracted. Subsequent 1 μL aliquots of an aqueous ligand solution (increasing in concentration from 0 to 5.43 μM , depending on the ligand affinity) were added to the solution containing RNA, and the fluorescence spectrum was recorded after the addition of each aliquot until the 2-AP fluorescence signal at 365 nm reached saturation (typically 5–10 min). Over the entire range of ligand concentrations, the emission maxima varied less than 1 nm. The total volume of the sample never changed more than 20%. The full titration was repeated in the absence of labeled RNA to correct for the presence of the ligand's fluorescence. These spectra were subtracted from each corresponding point of the labeled RNA titrations, and the resulting fluorescence intensity was corrected for dilution (FV/V_0). The emission fluorescence at 365 nm was normalized by dividing the difference between the observed fluorescence, F_{ob} , and the initial fluorescence, F_i , by the difference between the final fluorescence, F_f , and the initial fluorescence, F_i : $F_N = (F_{\text{ob}} - F_i)/(F_f - F_i)$. This normalized fluorescence intensity (F_N) was plotted as a function of the logarithm of the total ligand concentration. Finally, nonlinear regression using a sigmoidal dose–response curve was performed with the software package GraphPad Prism 4 (GraphPad Software, San Diego, CA) to calculate the EC_{50} values. Experimental errors were less than or equal to $\pm 25\%$ of each value.

NMR Spectroscopy of RNA–Ligand Complexes. NMR spectra were acquired with a Bruker Avance spectrometer operating at 600 MHz and equipped with a cryoprobe. Samples of the complexes were prepared by mixing the appropriate amounts of RNA and ligand and performing an annealing protocol consisting of heating to 90 $^\circ\text{C}$ for 3 min, followed by snap cooling on ice for 20 min. Samples were dissolved in 10 mM pH 6.8 sodium phosphate, in a 9/1 $\text{H}_2\text{O}/\text{D}_2\text{O}$ mixture, and NMR spectra were recorded at 5 $^\circ\text{C}$ to reduce the exchange with water. Water suppression was achieved by using an excitation sculpting sequence (zgesgp).

■ ASSOCIATED CONTENT

📄 Supporting Information

Figures giving 1D (^1H and ^{13}C) and 2D NMR spectra of all compounds synthesized, reversed-phase HPLC traces of the ligands, and fluorescence titration curves. This material is available free of charge via the Internet at <http://pubs.acs.org>.

■ AUTHOR INFORMATION

Corresponding Author

*E-mail for V.M.: vmarchan@ub.edu.

Notes

The authors declare no competing financial interest.

■ ACKNOWLEDGMENTS

We wish to thank Prof. Enrique Pedrosa for fruitful discussions on the design of Janus structures. This work was supported by funds from the Ministerio de Economía y Competitividad (CTQ2010-21567-C02-01), the Generalitat de Catalunya (2009SGR-208), and the Programa d'Intensificació de la Recerca (UB). G.A. was a recipient fellow of the University

of Barcelona. We acknowledge Dr. Margarida Gairí from the Barcelona Scientific Park for NMR technical support and Dr. Irene Fernández and Laura Ortiz from the facilities of the Servei d'Espectrometria de Masses of the University of Barcelona for MS support.

REFERENCES

- (1) (a) Zaman, G. J. R.; Michiels, P. J. A.; van Boeckel, C. A. A. *Drug Discov. Today* **2003**, *8*, 297. (b) Thomas, J. R.; Hergenrother, P. J. *Chem. Rev.* **2008**, *108*, 1171. (c) Aboul-ela, F. *Future Med. Chem.* **2010**, *2*, 93. (d) Guan, L.; Disney, M. D. *ACS Chem. Biol.* **2012**, *7*, 73.
- (2) (a) Stelzer, A. C.; Frank, A. T.; Kratz, J. D.; Swanson, M. D.; Gonzalez-Hernandez, M. J.; Lee, J.; Andricioaei, I.; Markovitz, D. M.; Al-Hashimi, M. *Nat. Chem. Biol.* **2011**, *7*, 553. (b) Ofori, L. O.; Hoskins, J.; Nakamori, M.; Thornton, C. A.; Miller, B. L. *Nucleic Acids Res.* **2012**, *40*, 6380. (c) Childs-Disney, J. L.; Parkesh, R.; Nakamori, M.; Thornton, C. A.; Disney, M. D. *ACS Chem. Biol.* **2012**, *7*, 1984. (d) Guan, L.; Disney, M. D. *Angew. Chem., Int. Ed.* **2013**, *52*, 1462.
- (3) Mounné, R.; Catala, M.; Larue, V.; Micouin, L.; Tisé, C. *Biochimie* **2012**, *94*, 1607.
- (4) Bryson, D. I.; Zhang, W.; McLendon, P. M.; Reineke, T. M.; Santos, W. L. *ACS Chem. Biol.* **2012**, *7*, 210.
- (5) (a) Varani, G.; McClain, W. H. *EMBO Rep.* **2000**, *1*, 18. (b) Xu, D.; Landon, T.; Greenbaum, N. L.; Fenley, M. O. *Nucleic Acids Res.* **2007**, *35*, 3836.
- (6) Hermann, T.; Westhof, E. *Chem. Biol.* **1999**, *6*, R335.
- (7) (a) Varnai, P.; Canalia, M.; Leroy, J.-L. *J. Am. Chem. Soc.* **2004**, *126*, 14659. (b) Lee, J.-H.; Pardi, A. *Nucleic Acids Res.* **2007**, *35*, 2965.
- (8) Branda, N.; Kurz, G.; Lehn, J.-M. *Chem. Commun.* **1996**, 2443.
- (9) (a) Chen, D.; Meena; Sharma, S. K.; McLaughlin, L. W. *J. Am. Chem. Soc.* **2004**, *126*, 70. (b) Chen, H.; Meena; McLaughlin, L. W. *J. Am. Chem. Soc.* **2008**, *130*, 13190. (c) Shin, D.; Tor, Y. *J. Am. Chem. Soc.* **2011**, *133*, 6926. (d) Zeng, Y.; Pratumyot, Y.; Piao, X.; Bong, D. J. *Am. Chem. Soc.* **2012**, *134*, 832.
- (10) (a) Arambula, J. F.; Ramisetty, S. R.; Baranger, A. M.; Zimmerman, S. C. *Proc. Natl. Acad. Sci. U.S.A.* **2009**, *106*, 16068. (b) Jahromi, A. H.; Nguyen, L.; Fu, Y.; Miller, K. A.; Baranger, A. M.; Zimmerman, S. C. *ACS Chem. Biol.* **2013**, *8*, 1037.
- (11) (a) López-Senín, P.; Gómez-Pinto, I.; Grandas, A.; Marchán, V. *Chem. Eur. J.* **2011**, *17*, 1946. (b) López-Senín, P.; Artigas, G.; Marchán, V. *Org. Biomol. Chem.* **2012**, *10*, 9243.
- (12) (a) Varani, L.; Hasegawa, M.; Spillantini, M. G.; Smith, M. J.; Murrell, J. R.; Ghetti, B.; Klug, A.; Goedert, M.; Varani, G. *Proc. Natl. Acad. Sci. U.S.A.* **1999**, *96*, 8229. (b) Donahue, C. P.; Muratore, C.; Wu, J. Y.; Kosik, K. S.; Wolfe, M. S. *J. Biol. Chem.* **2006**, *281*, 23302.
- (13) (a) Varani, L.; Spillantini, M. G.; Goedert, M.; Varani, G. *Nucleic Acids Res.* **2000**, *28*, 710. (b) Donahue, C. P.; Ni, J.; Rozners, E.; Glicksman, M. A.; Wolfe, M. S. *J. Biomol. Screening* **2007**, *12*, 789. (c) Zheng, S.; Chen, Y.; Donahue, C. P.; Wolfe, M. S.; Varani, G. *ACS Chem. Biol.* **2009**, *16*, 557. (d) Liu, Y.; Peacey, E.; Dickson, J.; Donahue, C. P.; Zheng, S.; Varani, G.; Wolfe, M. S. *J. Med. Chem.* **2009**, *52*, 6523.
- (14) (a) Spillantini, M. G.; Murrell, J. R.; Goedert, M.; Farlow, M. R.; Klug, A. *Proc. Natl. Acad. Sci. U.S.A.* **1998**, *95*, 7737. (b) Liu, F.; Gong, C. X. *Mol. Degener.* **2008**, *3*, 8. (c) Wolfe, M. S. *J. Biol. Chem.* **2009**, *284*, 6021.
- (15) (a) Fenniri, H.; Deng, B.-L.; Ribbe, A. E.; Hallenga, K.; Jacob, J.; Thiagarajan, P. *Proc. Natl. Acad. Sci. U.S.A.* **2002**, *99*, 6487. (b) Johnson, R. S.; Yamazaki, T.; Kovalenko, A.; Fenniri, H. *J. Am. Chem. Soc.* **2007**, *129*, 5735. (c) Tikhomirov, G.; Oderinde, M.; Makeiff, D.; Mansouri, A.; Lu, W.; Heirtzler, F.; Kwok, D. Y.; Fenniri, H. *J. Org. Chem.* **2008**, *73*, 4248.
- (16) (a) Beingessner, R. L.; Díaz, J. A.; Hemraz, U. D.; Fenniri, H. *Tetrahedron Lett.* **2011**, *52*, 661. (b) Takeda Pharmaceutical Company Limited, Patent US2011/152273A1, 2011. (c) Slavish, P. J.; Price, J. E.; Hanumesh, P.; Webb, T. R. *J. Comb. Chem.* **2010**, *12*, 807.
- (17) Von Angerer, S. Product class 12: pyrimidines. *Science of Synthesis* **2004**, *16*, 379.
- (18) Prystas, M.; Sorm, F. *Collect. Czech. Chem. Commun.* **1966**, *31*, 3990.
- (19) (a) Laliberté, D.; Maris, T.; Wuest, J. D. *J. Org. Chem.* **2004**, *69*, 1776. (b) Janczak, J.; Kubiak, R. *J. Mol. Struct.* **2005**, *749*, 60. (c) Asadi, A.; Patrick, B. O.; Perrin, D. M. *J. Org. Chem.* **2007**, *72*, 466.
- (20) Mittapalli, G. K.; Reddy, K. R.; Xiong, H.; Munoz, O.; Han, B.; De Riccardis, F.; Krishnamurthy, R.; Eschenmoser, A. *Angew. Chem., Int. Ed.* **2007**, *46*, 2470.
- (21) (a) Arya, D. P.; Xue, L.; Willis, B. J. *Am. Chem. Soc.* **2003**, *125*, 10148. (b) Blount, K. F.; Zhao, F.; Hermann, T.; Tor, Y. *J. Am. Chem. Soc.* **2005**, *127*, 9818.
- (22) (a) Houghton, J. L.; Green, K. D.; Chen, W.; Garneau-Tsodikova, S. *ChemBioChem* **2010**, *11*, 880. (b) Becker, B.; Cooper, M. A. *ACS Chem. Biol.* **2013**, *8*, 105.
- (23) (a) Luedtke, N. W.; Carmichael, P.; Tor, Y. *J. Am. Chem. Soc.* **2003**, *125*, 12374. (b) Luedtke, N. W.; Baker, T. J.; Goodman, M.; Tor, Y. *J. Am. Chem. Soc.* **2000**, *122*, 12035. (c) Staple, D. W.; Venditti, V.; Niccolai, N.; Elson-Schwab, L.; Tor, Y.; Butcher, S. E. *ChemBioChem* **2008**, *9*, 93.
- (24) Rabanal, F.; DeGrado, W. F.; Dutton, P. L. *Tetrahedron Lett.* **1996**, *37*, 1347.
- (25) Grau-Campistany, A.; Massaguer, A.; Carrion-Salip, D.; Barragán, F.; Artigas, G.; López-Senín, P.; Moreno, V.; Marchán, V. *Mol. Pharmaceutics* **2013**, *10*, 1964.
- (26) (a) Warui, D. M.; Baranger, A. M. *J. Med. Chem.* **2009**, *52*, 5462. (b) Llano-Sotelo, B.; Chow, C. S. *Bioorg. Med. Chem. Lett.* **1999**, *9*, 213–216.
- (27) Blakeley, B. D.; DePorter, S. M.; Mohan, U.; Burai, R.; Tolbert, B. S.; McNaughton, B. R. *Tetrahedron* **2012**, *68*, 8837.
- (28) Sproat, B. S. In *Oligonucleotide Synthesis: Methods and Applications*; Herdewijn, P., Ed.; Humana Press: Totowa, NJ, 2005; Methods in Molecular Biology 288, pp 17–31.